Cell Reports

Resource

A transcriptional atlas identifies key regulators and networks for the development of spike tissues in barley

Graphical abstract

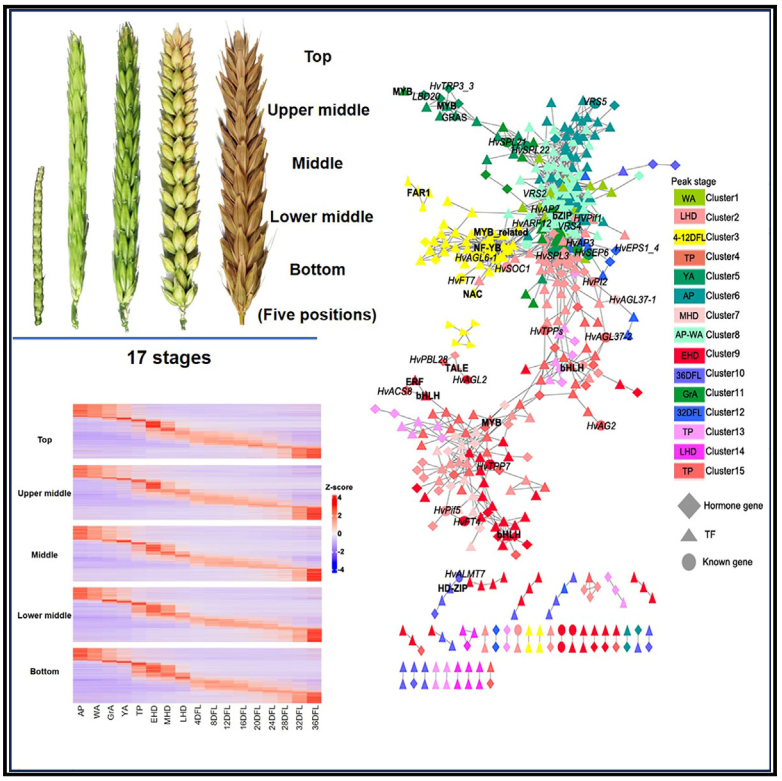

Highlights

- The transcriptome atlas includes 255 samples at 17 stages and 5 spikelet positions
- The temporal transcriptome dissects the floret initiation and development process
- The spatial transcriptome shows unbalanced development among the 5 positions

Authors

Liping Shen, Yangyang Liu, Lili Zhang, ..., Yuannian Jiao, Kuocheng Shen, Zifeng Guo

Correspondence

guozifeng@ibcas.ac.cn

In brief

Shen et al. develop a high-resolution spatiotemporal transcriptome atlas (255 samples) across 17 spike developmental stages and 5 spikelet positions in barley (*Hordeum vulgare*). The authors link transcriptional signatures to spike development and morphology. They identify a GDSL esterase/lipase gene as a regulator of spike morphology in barley.

Shen et al., 2023, Cell Reports *42*, 113441
November 28, 2023
https://doi.org/10.1016/j.celrep.2023.113441

CellPress

Cell Reports

CellPress
OPEN ACCESS

Resource

A transcriptional atlas identifies key regulators and networks for the development of spike tissues in barley

Liping Shen,[1,4,5] Yangyang Liu,[1,2,5] Lili Zhang,[1] Zhiwen Sun,[1,2] Ziying Wang,[1,2] Yuannian Jiao,[2,3] Kuocheng Shen,[1,2] and Zifeng Guo[1,2,4,6,*]

[1]Key Laboratory of Plant Molecular Physiology, Institute of Botany, Chinese Academy of Sciences, Beijing 100093, China
[2]University of Chinese Academy of Sciences, Beijing 100049, China
[3]State Key Laboratory of Systematic and Evolutionary Botany, Institute of Botany, the Chinese Academy of Sciences, Beijing 100093, China
[4]China National Botanical Garden, Beijing 100093, China
[5]These authors contributed equally
[6]Lead contact
*Correspondence: guozifeng@ibcas.ac.cn
https://doi.org/10.1016/j.celrep.2023.113441

SUMMARY

Grain number and size determine grain yield in crops and are closely associated with spikelet fertility and grain filling in barley (*Hordeum vulgare*). Abortion of spikelet primordia within individual barley spikes causes a 30%–50% loss in the potential number of grains during development from the awn primordium stage to the tipping stage, after that grain filling is the primary factor regulating grain size. To identify transcriptional signatures associated with spike development, we use a six-rowed barley cultivar (Morex) to develop a spatiotemporal transcriptome atlas containing 255 samples covering 17 stages and 5 positions along the spike. We identify several fundamental regulatory networks, in addition to key regulators of spike development and morphology. Specifically, we show *HvGELP96*, encoding a GDSL domain-containing protein, as a regulator of spikelet fertility and grain number. Our transcriptional atlas offers a powerful resource to answer fundamental questions in spikelet development and degeneration in barley.

INTRODUCTION

In members of the grass family such as cereals, inflorescences display a wide variety of architectures. In temperate cereal crops, the grain-bearing inflorescences are known as spikes, which consist of several spikelets. An individual spikelet is composed of one or more florets, which include the floral organs, e.g., lemma, palea, lodicules, stamens, and carpels. Arranged along the spike of barley (*Hordeum vulgare*) plant inflorescences are rachis nodes (Figure 1A), each being composed of a triplet structure with one central spikelet and two lateral spikelets. Depending on the fertility of the two lateral spikelets, each rachis node will bear either two-rowed or six-rowed spikes. In wild barley (*H. vulgare* ssp. *spontaneum*), the progenitor of modern-day cultivated barley, each rachis carries one fertile central spikelet and two sterile lateral spikelets, forming a two-rowed spike. In modern-day six-rowed barley cultivars, all three spikelets are fully fertile and can develop into grains at each rachis node. Six-rowed barley arose about 8,000–12,000 years ago during barley domestication by human selection of spontaneous recessive variants having the six-rowed phenotype.[1,2] Barley row type is determined at the early spike developmental stage, which is the stage following production of the maximum number of spikelet primordia.

Spike development is complex and determines the morphology of the spike at physiological maturity. The grain number and spikelet node number are closely associated with the survival rate of spikelet primordia per spike after the awn primordium (AP) stage, as nearly 30%–50% spikelet primordia within an individual spike will spontaneously abort.[3–6] In particular, the degeneration of apical spikelet primordia causes the largest loss in potential grain number. Grain filling after the tipping stage is the primary factor that regulates grain size in barley.

Here, we used Morex, a six-rowed barley cultivar whose whole-genome sequence is available,[7,8] to conduct a spatial-temporal transcriptome analysis to monitor spikelet development and degeneration in barley. Due to the uneven development of the top, middle, and bottom positions in the barley spike, we divided the spike from top to bottom into five positions. This division into five parts can accurately show the developmental differences of each node along the spike. The developmental period we studied comprised the AP stage to full maturity of the grain,[9–11] covering the entirety of spike development. Our spatiotemporal transcriptome atlas (255 samples at 17 stages and 5 positions along the spike) linked spike morphology to spikelet development and identified regulators and networks of spikelet development and degeneration. Using this

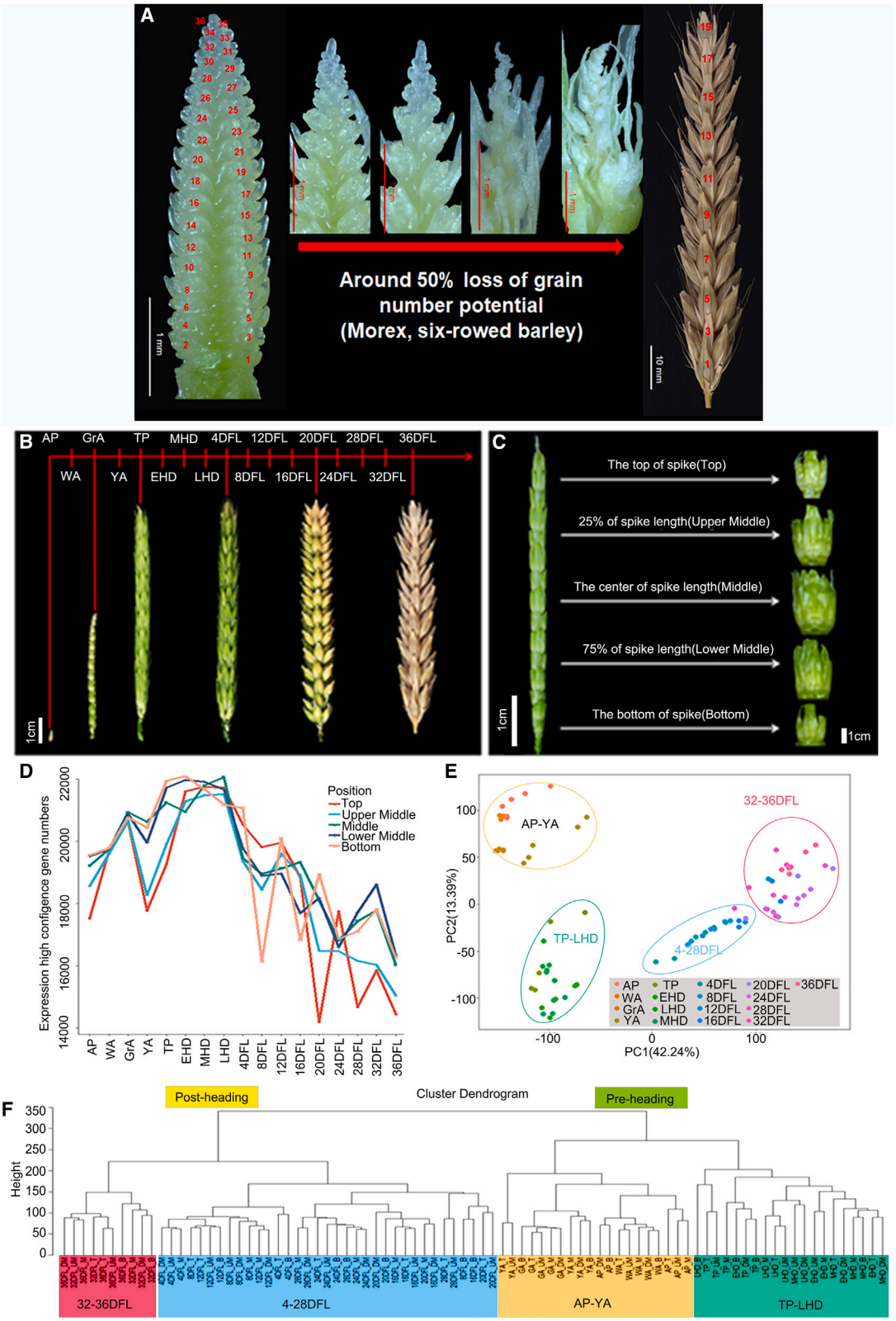

(legend on next page)

transcriptome atlas, we identified *HvGELP96*, a gene that encodes a GDSL esterase/lipase. It was highly expressed in the AP-YA (yellow anther) stage and can regulate spikelet fertility and grain number. This transcriptional atlas provides a comprehensive spikelet position- and stage-specific description of genome-wide transcriptional activity during spikelet development and degeneration, and should serve as a valuable future resource for understanding, and possibly manipulating, the genetic control of grain number and size in barley.

RESULTS

A spatiotemporal transcriptome atlas of spike development in six-rowed barley

Grain number and size are closely associated with spikelet development in barley. The spikelets at different positions along an individual spike display different degrees of development (Figures 1A–1C). Generally, the central spikelets grow more rapidly and are more advanced than apical and basal spikelets (Figures 1B and 1C). Notably, before grain setting at physiological maturity, the abortion of apical spikelet primordia within individual spikes results in a 30%–50% loss in the potential number of grains (Figure 1A).

To determine gene expression profiles during spikelet and spike development, we used a transcriptome deep sequencing (RNA-seq) approach in samples representing 17 developmental stages: the AP stage, the white anther stage, the green anther (GrA) stage, the YA stage, the tipping (TP) stage, the early heading (EHD) stage (20%–30% of individual spikes visible), the middle heading (MHD) stage (50% of individual spikes visible), and the late heading (LHD) stage (more than 90% of individual spikes visible), in addition to stages representing 4 days following late heading (4, 8, 12, 16, 20, 24, 28, 32, and 36 DFL) (Figure 1B). To assess differences in expression at different stages of spikelet development within individual spikes, we also performed an RNA-seq analysis of spikelets using samples collected at one of five positions along individual spikes: spikelets at the top of the spike (top), the top 25% of the spike (upper middle), the center of the spike (middle), the top 75% of the spike (lower middle), and the bottom of the spike (bottom) (Figure 1C). We reasoned that this spatiotemporal gene expression dataset of spikelets at 17 stages and 5 positions would allow us to dissect the dynamics and differences in gene expression across stages during spikelet development and subsequent degeneration of some spikelets.

In this study, we used 3 biological replicates for each tissue, resulting in 255 (17 stages × 5 positions × 3 replicates) highly tissue-specific and informative samples for RNA-seq analysis. In total, we mapped 6.21 billion high-quality reads to the Morex reference genome.[8] The mapping ratio to the reference genome ranged from 76% to 90% (Table S1); we only used uniquely mapped reads to calculate normalized gene expression levels (as transcripts per kilobase million [TPM]). We calculated the average TPM values across the three replicates to estimate gene expression levels in all samples. To minimize the effect of transcriptional noise, we defined a gene as expressed if its mean TPM value was greater than 1. In total, we considered 30,041 genes as being expressed in at least one of the 85 tissues (5 positions × 17 stages), including 1,454 transcription factor (TF) genes (Table S2).

To investigate changes in gene expression in different parts of the barley spike at different developmental stages, we determined the number of genes expressed in different parts of the spike at the same stage. The number of genes expressed in each of the five parts showed the same trend, with the number of genes detected in the TP-LHD stage being much higher than the number detected in the AP-YA and 4–36 DFL stages. An analysis of the spatial expression profile of genes revealed that the number of expressed genes in the five parts of the spikelet differ less during the TP-LHD developmental window than during the AP-YA and 4–36 DFL windows. After pollination (TP-LHD), the number of expressed genes decreased sharply, and we observed a greater difference in the number of expressed genes between the top and bottom parts of the spike (Figure 1D; Table S3). The identification of genes specifically expressed at different spikelet positions indicated that the expression patterns of genes for early flower forming, pollination, and late seed storage change dramatically during spike development, with uneven gene expression levels at different positions of the spike. Principal-component analysis (PCA) (Figure 1E) and hierarchical clustering analysis (Figure 1F) of all 85 samples showed a clear distinction among AP-YA, TP-LHD, and 4–28 and 3–36 DFL windows, indicating that different transcriptional pathways are likely activated during the different developmental stages of spikelets.

Temporal transcriptome analysis identifies regulators for various events during spike development

An analysis of gene expression profiles across the 5 parts of the spike revealed that gene expression in the spike exhibits temporal specificity, with genes expressed in the 5 parts showing approximately the same expression trend (Figure 2A). We identified 9,228 genes expressed in all 5 parts of the spike, prompting

Figure 1. Spatiotemporal dissection of spike development in six-rowed barley, cultivar Morex

(A) Spikelet primordium abortion (at the top of the spike) occurs between the AP stage (left) and physiological maturity (right). The image on the left shows 36 developing spikelet nodes for a spike at the AP stage (the stage having the maximum number of spikelet nodes) and 19 spikelet nodes for the spike at physiological maturity on the right.

(B) Diagram of barley spike samples collected at time points representing 17 spike developmental stages used for transcriptome analysis.

(C) Spikelet samples at five positions used for transcriptome analysis.

(D) High-confidence gene expression in each of the five spike parts during spike development.

(E) Principal-component analysis (PCA) of the transcriptomes of the samples at the 17 time points.

(F) Cluster dendrogram analysis of RNA-seq data showing four distinct developmental windows in the pre-heading and post-heading stages: AP-YA (pre-heading stages), TP-LHD (pre-heading stages), 4–26 DFL (post-heading stages), 32–36 DFL (post-heading stages). AP, awn primordium stage; WA, white anther stage; GrA, green anther stage; YA, yellow anther stage; TP, tipping stage; EHD, early heading stage; MHD, middle heading stage; LHD, late heading stage; DFL, day after late heading.

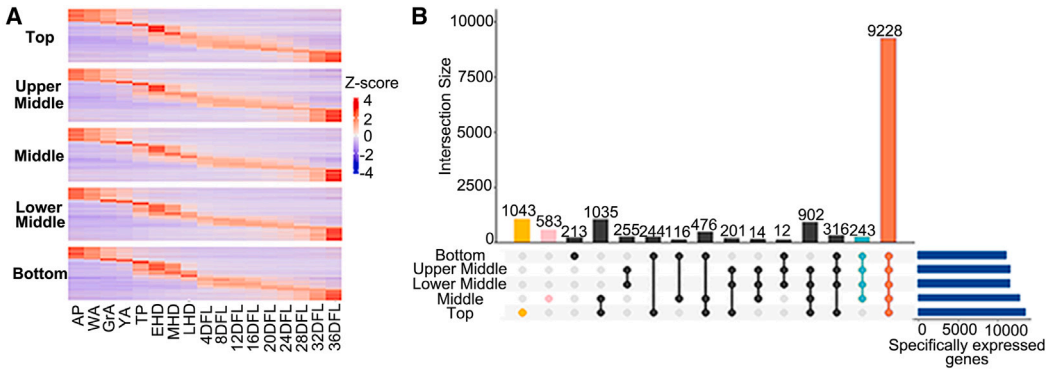

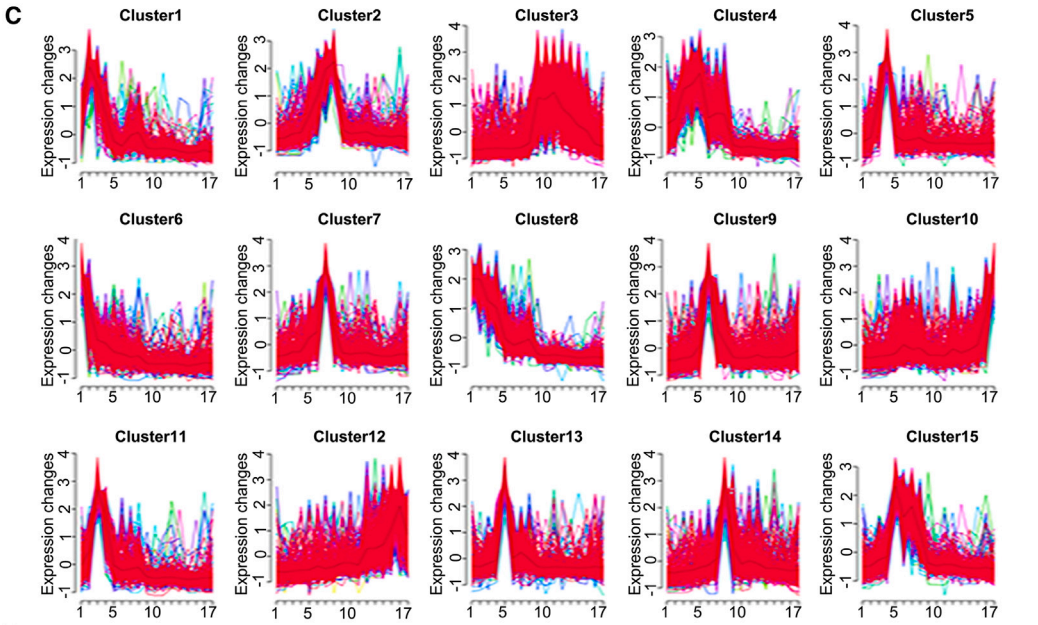

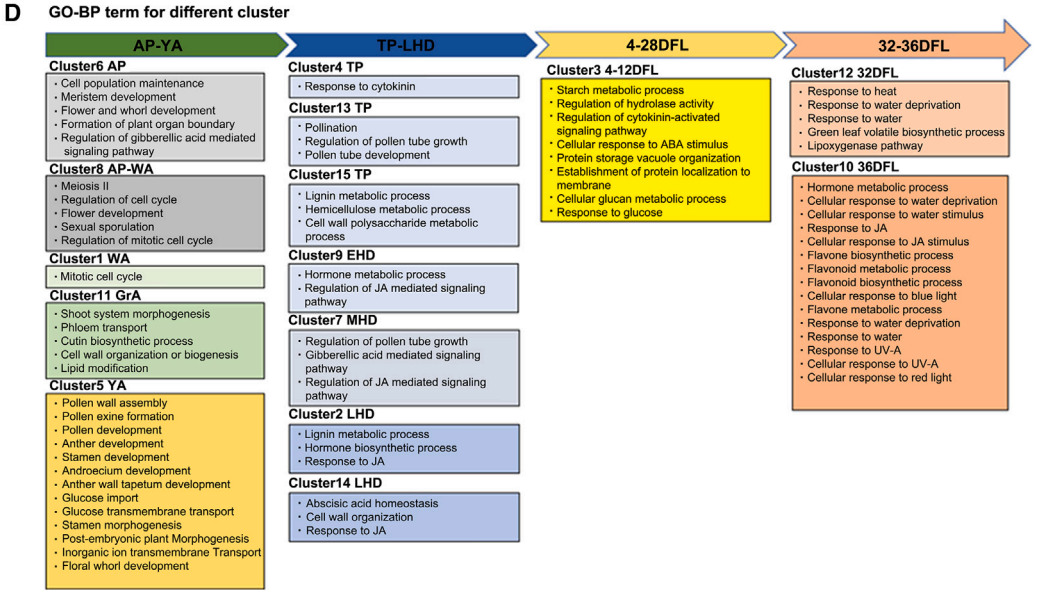

(legend on next page)

us to hypothesize that they are involved in normal spike development (Figure 2B). A dynamic expression pattern for genes will reflect their role in spikelet development. Overlapping or common pathways can often be revealed by identifying the sets of genes showing different or similar expression patterns. To this end, we applied a fuzzy c-means algorithm[12] to group the 9,228 above genes. We performed this analysis for the middle spikelets, which show fuller development compared with the other positions. We detected 15 clusters, representing genes with different temporal expression patterns (Figure 2C; Tables S4 and S5). This observation indicated that different kinetics of gene expression characterize the changes in transcript abundance at each stage in relation to spike transcriptional activation. We noticed that genes in clusters 2 and 14 are highly expressed in the LHD stage, whereas genes in clusters 4, 13, and 15 were highly expressed in the TP stage. Using the results from PCA and hierarchical clustering analysis, we determined that the genes from clusters 1, 5, 6, 8, and 11 are highly expressed during the AP-YA stages, whereas the genes in clusters 2, 4, 7, 9, 13, 14, and 15 reached a peak in expression during the TP-LHD stages. Only three clusters (3, 10, 12) had genes with peaks in expression during the post-heading stages, with genes from cluster 3 reaching a peak at 4–28 DFL, genes from cluster 12 at 32 DFL, and genes from cluster 10 at 36 DFL. These results suggest that gene expression patterns are complex and diverse during early spike development and that these genes are more likely to interact with each other.

The sets of genes in clusters 1, 5, 6, 8, and 11 with peak expression levels during the AP-YA window are likely to represent genes expressed during the major phase of flower organ development (Figures 1F and 2C). This developmental stage is characterized by the completion of meiosis, from the time when the initiation of all spikelet structures is complete to the time when the polar gradually grows and completely envelops the stamens and carpels.[11] Gene ontology (GO) term enrichment analysis showed that the AP-YA stage is associated with genes involved in meiosis and flower organ formation, as well as with gene-related phytohormones such as gibberellin (GA), jasmonic acid (JA), and auxin (Figure 2D; Table S6). Among genes from cluster 6, we noted auxin response factors (ARFs), YABBY4, a homolog of snapdragon (*Antirrhinum majus*) FLORICAULA (FLO) and Arabidopsis (*Arabidopsis thaliana*) LEAFY (LFY), and SQUAMOSA PROMOTER BINDING-LIKE PROTEINs (SPL2, SPL7, SPL17). ARF and LFY are TFs involved in flower development, floral organ development, floral whorl development, and floral meristem determinacy, with LFY being also involved in the maintenance of stem cell populations[13–15] (Table S6). GO terms associated with genes in cluster 8 were "meiosis," cell cycle," "regulation of the metaphase/anaphase transition in the cell cycle," and "sexual sporulation" (Table S6). PAIRING ABERRATION IN RICE MEIOSIS1 (PAIR1) is essential for the establishment of homologous chromosome pairing during meiosis in rice (*Oryza sativa*),[16] and HORMA domain-containing protein 1 is associated with the meiotic chromosome axis.[17] We identified a barley homolog to PAIR1 and a barley homolog to human HORMA domain-containing protein 1 (HORMAD1) in most GO categories related to reproductive sporogenesis development and meiosis (Table S6). *HvMADS32* is a putative ortholog of *OsMADS32*, which encodes an important transcription factor for maintaining floral meristem identity that integrates the action of other MADS-box homeotic proteins to sustain floral organ specification and development in rice.[18] *Epidermal patterning factor-like1* (*TaEPFL1*) from wheat (*Triticum aestivum*) was previously shown to be highly expressed in pistillody stamens, and overexpression of *TaEPFL1* leads to abnormal stamens.[19] We also detected a putative barley ortholog to *TaEPFL1*, *HvEPFL1*, in cluster 5, showing an abnormally high level.

Members of the *SPL* family, whose transcripts are targets of microRNAs from the miR156 family, are unique to plants and are involved in many aspects of plant development.[20] We detected the expression of *SPL* family members, including *HvSPL8*, *HvSPL17*, *HvSPL21*, and *HvSPL22*, during the AP-YA stage. *SPL8* affects the early stages of microsporogenesis and megasporogenesis in Arabidopsis,[21] with is in line with the developmental events occurring in the AP-YA stages in barley.[11] We also observed an enrichment for ABCDE model genes underlying flower development, including the B-class gene *APETALA 3* (*HvAP3*), the E-class genes *HvMADS1*, *SEPALLATA 5* (*HvSEP5*), and *HvSEP6*. In Arabidopsis, *AP3* is specifically expressed in petals and stamens, and *AP3* and C-class genes work together to regulate stamen development.[22,23] The *SEP* genes are expressed together with the ABC genes and participate in the transition from vegetative to floral organs.[24] HvMADS1 regulates cytokinin homeostasis to maintain an unbranched spike architecture at high temperature.[25] We also identified the AP2-like genes, *HvAP2L5* and *HvAP2L7*, during the AP-YA stage; *AP2L5* plays a critical role in the specification of axillary floral meristems and lemma identity in wheat.[26]

The genes from clusters 2, 4, 7, 9, 13, 14, and 15 showed an expression peak between stages TP and LHD, and likely represent genes related to flowering and pollination in barley. At this stage, the awn first emerges from the leaf sheath, followed by emergence of the spike.[27] We identified genes involved in most of the phytohormone-related pathways during this phase, such as response to cytokinins, regulation of JA-mediated signaling pathways, GA-mediated signaling pathways, and abscisic acid (ABA) homeostasis (Figure 2D; Table S6). Genes associated with GO terms related to pollen tube formation in

Figure 2. Composition of the transcriptome at 17 developmental stages and 5 spikelet positions

(A) Heatmap representation of gene expression levels during the AP to 36DFL transition at five spikelet positions.

(B) Number of genes expressed at each of the five spikelet positions. Specifically, the x axis defines the total number of differentially expressed genes (DEGs) identified at each spikelet position, while the y axis provides the number of DEGs unique to each set of DEGs across different positions.

(C) Fifteen clusters for the 9,228 genes (expressed in all 5 spikelet positions) with different expression patterns across the 17 developmental stages. For each cluster, one line represents an individual gene, yellow or green lines indicate genes with low values of membership; red and purple lines indicate genes with high values of membership.

(D) Gene ontology (GO) terms associated with genes in the 15 clusters.

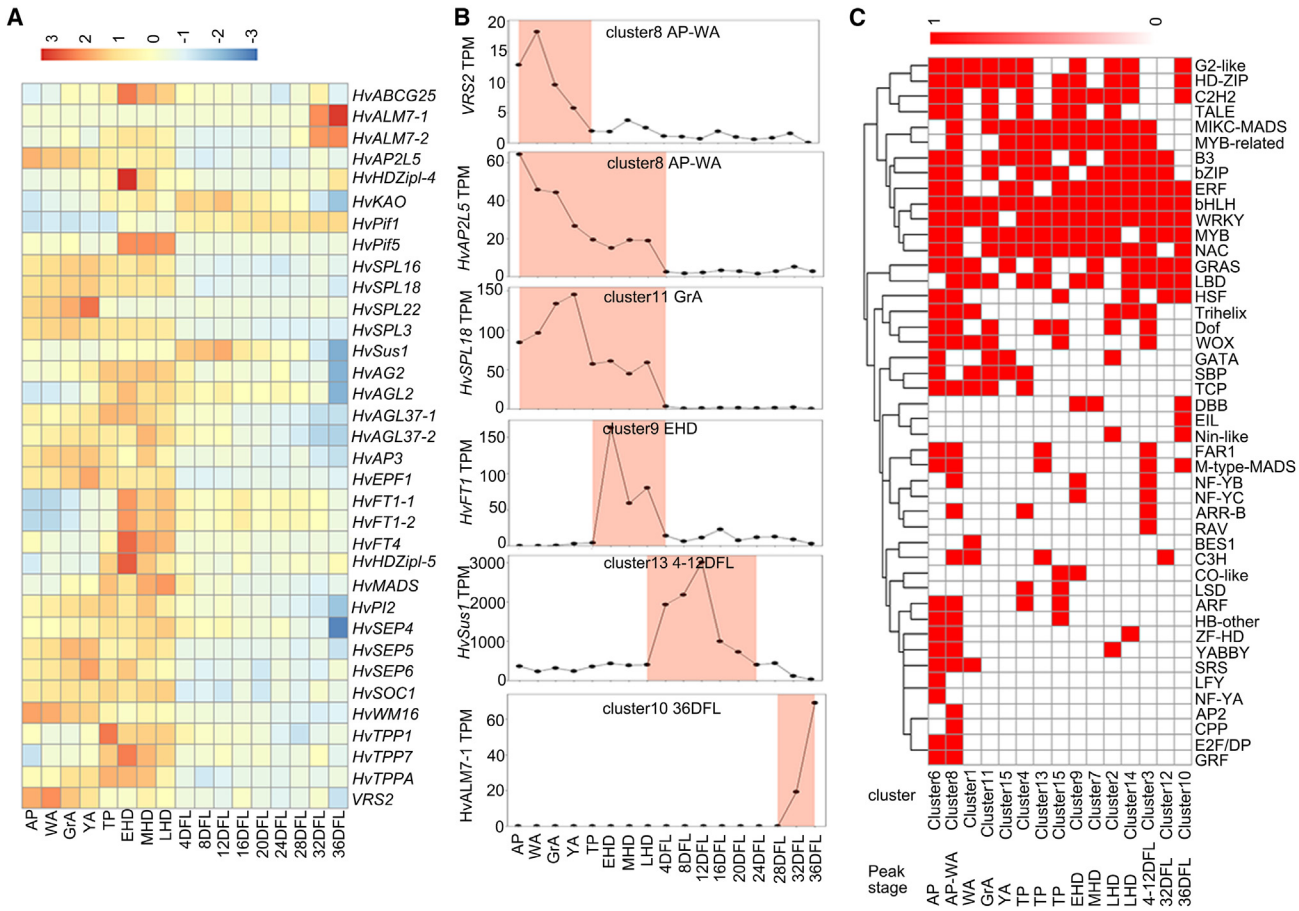

Figure 3. Expression patterns of different TF genes and other genes during spike development

(A) Heatmap representation of the expression of genes belonging to different clusters across the 17 developmental stages. The color key at the top shows normalized TPM values for relative gene expression.

(B) Expression patterns of 6 representative genes shown in (A) across the 17 developmental stages. The colored regions highlight the peaks in gene expression.

(C) Peak stages of different families of TF genes from the 15 clusters. A value of 1 indicates that a TF gene was identified in the cluster, 0 indicates that it was not identified.

clusters 13 and 7 had high expression in the TP and MHD stages (Figure 2D; Table S6). During this period, we detected the expression of *FLOWERING LOCUS T* (*FT*) genes (*HvFT1* and *HvFT4*) and *CENTRORADIALIS* (*HvCEN*) (Table S5). The barley genome harbors 12 known *FT*-like genes in barley, of which *HvFT1* is the main *FT*-like gene involved in flowering, with *HvFT2* and *HvFT4* being expressed later in development.[28] *HvFT4* was previously shown to regulate flowering time and floret fertility.[29] *CEN* is a key regulator of flowering time and inflorescence architecture in plants, and HvCEN interacts with HvFT1 to repress floral development under short day photoperiods.[30] These results suggest that *FT* genes and *CEN* regulate spikelet development in the TP-LHD window in barley.

MADS-box genes are master regulators of floral structures; *PISTILLATA* (*PI*) is a class B gene in the ABC model, regulating the formation of petals and stamens, while *AGAMOUS* (*AG*) is a C-class gene that regulates the development of stamens and pistils in Arabidopsis.[31] Expression of some *MADS* family genes, including *HvPI2*, *HvAG2*, *HvSEP4*, *HvAGL2*, *HvAGL37*, *HvAGL37-2*, and *HvSOC1*, was prevalent during the TP-LHD stages (Figure 3A; Tables S4 and S5). *SEP4* works together with other *SEP*s; a *sep1 sep2 sep3 sep4* quadruple mutant in Arabidopsis exhibits a conversion of floral organs into leaf-like organs.[32] *AGAMOUS-LIKE 2* (*AGL2*) is expressed in all four whorls of the flower and plays a fundamental role in the development of all floral organs.[33] *SUPPRESSOR OF OVEREXPRESSION OF CO 1* (*SOC1*) is regulated by two antagonistic flowering regulators, and *CONSTANS* and *FLOWERING LOCUS C* (*FLC*) act as a general regulators in organogenesis.[34] Overall, these results suggest that the TP-LHD period is also an important time for organ development, as *MADS* genes play an important function in the stage and many are highly expressed in barley spikelets.

The differentially expressed genes (DEGs) at this stage (TP-LHD) included members of the trehalose 6-phosphate phosphatase (TPP) gene family, such as *HvTPP1-1*, *HvTPP1-2*, *HvTPP1-3*, and *HvTPP7* (Tables S4 and S5). TPP proteins regulate and reprogram carbon metabolism in the light, and can improve drought tolerance in plants. *AtTPPI* enhances drought

tolerance by regulating stomatal aperture in Arabidopsis,[35] while *OsTPP7* increases tolerance to anaerobic germination in rice.[36] Thirty-two homeodomain leucine zipper (*HD-Zip*) genes (*HvHD-Zip 1–32*) are present in the barley genome and play an important role in plant growth and environmental responses.[37] *HvHDZipI-4* and *HvHDZipI-5* were highly expressed in the period between the TP and LHD stages. These results suggest that this stage may also be a critical period for tolerance to adverse growth conditions in spikelets. Two phytohormone-related genes, one encoding the brassinosteroid (BR) receptor BR-insensitive 1 (HvBRI1) and one encoding the ABA exporter HvABCG25, were specifically highly expressed (Tables S4 and S5), suggesting that ABA and BR signaling pathways contribute to spikelet development at this stage.

The expression peak of genes from cluster 3 was in the 4–28 DFL stage (Figure 2D), corresponding to the period of seed development and grouting. SUS1, a sucrose synthase, catalyzes the reaction between sucrose and UDP to form UDP-glucose and fructose and regulates the level of sucrose in plants.[38] SUS1 can affect endosperm filling in maize (*Zea mays*)[39] and is associated with the thousand-kernel weight of wheat grains.[40] The timing of *SUS1* expression was consistent with the biological events occurring in this period (Figure 3B; Table S4). *HvAGL6-1* and *HvAGL6-2* genes were also highly expressed at this stage (Figure 3A; Table S4). *AGL6* is highly expressed in ovules, lodicules, paleas, and floral meristems, and directly regulates *FACTOR OF DNA METHYLATION LIKE1* (*FDML1*) to affect flower development in rice.[41] In wheat, *TaAGL6* regulates the expression of *TaAP3* to affect stamen development.[42] Because of its high expression level during the period of 4–28 DFL, we conclude that *AGL6* may influence the development of spikelets after fertilization in barley.

As the endosperm is an important storage organ for starch and protein in wheat seeds, we hypothesized that some of the products encoded by highly expressed genes at this stage store nutrients by inhibiting catabolic enzymatic activity to prevent them from being degraded. Some GO biological process terms were indeed associated with starch and glucose, such as starch metabolic process, cellular glucan metabolic process, and response to glucose (Figure 2D; Table S6). GO molecular function classification of cluster 3 genes suggested inhibition of various proteolytic reactions, for example, serine-type endopeptidase inhibitor activity, which delays protein degradation and has both peptidase inhibitor activity and endopeptidase inhibitor activity.[43,44] Programmed cell death in seeds was reported to correlate with increased seed-filling rate and grain weight, and mainly occurs 5–13 days after anthesis.[43] We noticed a number of peroxidase genes in this cluster (Table S4); these genes may be linked to programmed cell death in barley starch endosperm.[45,46]

The genes in clusters 10 and 12 were highly expressed during spikelet maturation and dehydration (32–36 DFL). Seed tolerance to dehydration is derived from a combination of characteristics acquired during seed development, and is accompanied by seed dehydration at a later stage of development. Seed tolerance to dehydration is linked to phytohormonal and antioxidant enzyme systems. During this stage, we identified 27 genes encoding late embryogenesis-abundant (LEA) proteins (Table S4), which are involved in protecting land plants from damage caused by environmental stresses, especially dehydration during drought conditions.[47] The presence of *LEA*s is consistent with the GO terms for response to water deficit (Table S6).

Spatial transcriptome analysis identifies regulators of differential spikelet development in individual spikes

To identify regulators of differential spikelet development at different positions, we looked for genes expressed in a position-specific manner. Spikelets in the top position had the highest number of DEGs, whereas those in the bottom position had the fewest. Overlap of genes among the five spikelet positions accounted for 61.0% (9,228/15,127) of the detected genes. Notably, we detected no gene specifically expressed in the upper-middle or lower-middle spikelet positions; of all DEGs, 6.9% (1,043 genes) were specific for the top spikelet position, with another 3.85% (583 genes) being specific for the middle spikelet position and 1.4% (213 genes) specific for the bottom position (Figures 2B and S1; Table S7).

Several genes encoding senescence-associated proteins were highly expressed in the top spikelet position; these genes may be directly related to the observed spikelet abortion that occurs at the top of the spike (Figure S1). In addition, among the DEGs in the apical spikelets, genes related to the auxin and BR pathways were significantly enriched (Table S8). Auxin is a key phytohormone in plant growth and development; enriched auxin pathway genes in the apical spikelets included *INDOLE-3-ACETIC ACID INDUCIBLE 21* (*HvIAA21*), *HvIAA18*, *HvARF10*, and *GRETCHEN HAGEN 3.2* (*HvGH3.2*). The AUX/IAA family includes early response proteins that can regulate the expression of auxin response genes by specifically binding to ARFs, which are transcriptional activators of auxin-responsive target genes and are essential for regulating auxin signaling throughout the plant life cycle.[48,49] *GH3* genes encode acyl acid amidosynthetases, which catalyze conjugation reactions of salicylic acid, JA, and auxin with amino acids,[50] suggesting that auxin plays an important role in the development and degradation of the top spikelets.

BRs are plant steroid hormones that play important roles in plant growth and development.[51] Brassinazole-resistant 1 (BZR1) is a core component of the BR signal transduction pathway in Arabidopsis. After being activated by a BR signal, BZR1 binds to the promoter region of downstream target genes to regulate their expression.[52] In this study, *HvBZR1* was specifically expressed at the top of the spike (Table S8). Previous studies on the function of BRs have mainly focused on accelerating crop growth and increasing crop yield[53]; the results presented here indicate that BRs regulate apical spikelet development and abortion, which influences grain number and size.

DEGs in the top position also included the *LATERAL ORGAN BOUNDARIES* (*LOB*) genes *HvLBD26* and *HvLBD37* (Table S8). *LBD* genes encode plant-specific TFs that have conserved LOB domains, which are involved in crosstalk between different signaling pathways. LBD proteins regulate a large number of developmental and metabolic programs in land plants, such as meristem programming, inflorescence development, lateral root formation, vascular patterning, anthocyanin biosynthesis, and nitrogen metabolism.[54,55] LOB family genes are also involved in the development of lateral organs.[54] The LOB genes

that were specifically expressed at the top of the spike may have new functions and are candidates for subsequent exploration.

Nitrate transporter 1 (NRT1)/peptide transporter family proteins were originally identified as nitrate or di/tri-peptide transporters. Members of this family transport auxin, ABA, and GAs, as well as secondary metabolites such as glucosinolates.[56] In this study, we detected the specific expression of one *NRT1/PTF* gene (*HvNRT1.9*) at the top of the spike (Table S8). We speculate that this *NRT1/PTR* gene may regulate the development of apical spikelets by coordinating the action of various phytohormones. Small auxin upregulated RNA (SAUR) proteins are involved in a wide range of cellular, physiological, and developmental programs involving phytohormonal and environmental control of plant growth and development,[57] and the SAUR-like auxin-responsive gene *HvSAUR61* was also a DEG in the apical spikelet and may regulate the development and degeneration of the spike apex in barley.

The DEGs at the basal spikelet included the GA pathway gene *GIBBERELLIN 2-OXIDASE 1* (*HvGA2ox1*) and the auxin pathway genes *HvARF10* and *PIN-FORMED 5* (*HvPIN5*) (Table S8). GA2oxs catalyze the formation of an inactive GA form in plants. Auxin can interact with GAs by upregulating *GA20ox* and *GA3ox* expression, while also downregulating *GA2ox* expression.[58] PIN5 belongs to a functionally uncharacterized subclade of PIN proteins, which are auxin transporters required for auxin-mediated development.[59] Previous studies have shown that the GA content in the top and bottom positions of barley spikes was lower than in the middle position, while the content of auxin is higher at the bottom of the spike[60]; this differential distribution of GAs and auxin may be related to a high expression level of the above genes.

The cytokinin pathway gene *HvCKX2* and two auxin pathway genes, *HvGH3.2* and *HvIAA7*, were DEGs in the top and bottom positions (Table S8). Cytokinins can control growth and cell division, and cytokinin oxidase 2 (CKX2) is a member of a family of enzymes involved in cytokinin catabolism. This result is consistent with the previously reported graded distribution of auxin and cytokinins in barley spikes.[60] The top and bottom positions of barley spikes undergo spikelet degradation, and the auxin and cytokinin phytohormone pathways may be involved in these stages. Identification of DEGs in the five positions provides a useful resource to understand the differential development occurring in the different spikelet positions.

Co-expression analysis of genes involved in spike development

The identification of known genes and phytohormone-related genes in the 15 clusters defined above revealed that genes related to the transition from vegetative to flowering (*HvSPL3*, *HvSPL16*, *HvSPL18*, *HvSPL22*), and related to anthesis (*HvFT1-1*, *HvFT1-2*, *HvFT4*), sugar transport (*HvSUS1*), or stress (aluminium-activated malate transporter, *HvALM7-1* and *HvALM7-2*) were highly expressed during the AP-YA, EHD-LHD, and 4–12 and 32–36 DFL windows, respectively (Figures 3A and 3B; Table S9). These results demonstrate the reliability of our gene classification in the 15 clusters. Most of these known genes were highly expressed mainly prior to pollination (Figure 3A). The expression of inducible genes in plants is largely regulated at the transcriptional level by specific TFs and phytohormones. We thus analyzed TF- and phytohormone-related genes separately and identified 193 phytohormone-related genes and 670 TF genes (Table S4). The 670 TF genes identified in the 15 clusters were grouped into 46 categories. Enrichment analysis of the TFs showed that TCP TFs were significantly enriched ($p < 0.05$) in cluster 1, and NAC-, FAR1-, and MYB-related TFs were significantly enriched ($p < 0.05$) in cluster 3. Significant enrichment ($p < 0.05$) for GO term "SBP TFs" were observed in clusters 5 and 11, while significant enrichment ($p < 0.05$) for GO term "ERF TFs" were detected in clusters 9 and 12 (Table S10). The enrichment analyses of TFs indicated that most of the TFs were cluster specific.

TF genes subsequently used for analysis included members from the GRF, E2F/DP, AP2, NF-YA, LFY, and YABBY families (Figure 3C), which are associated with androgynophore development and morphological establishment of organs.[61,62] At the AP stage, the embryo spike has its full complement of spikelet primordia, and the initiation of all the structures within the central spikelet of the spike is complete. At this stage, we identified the TF gene *LFY* (Figure 3C), which initiates the floral gene expression program and is a key TF gene in floral organ development.[63,64] We identified genes encoding GRF TFs in clusters 6 and 8, including a GRF-interaction factor (*GIF*) gene in cluster 6 (Figure 3C). *GIF*s encode transcriptional co-activators that form a transcriptional complex with GRFs, involved in the maintenance of organoid meristemoid cells reproduction and regulating organ size by activating cell production and influencing cell number.[65–68] Some TF genes, such as *CO-like*, *DBB*, *NF-YB*, and *NF-YC*, were highly expressed during the flowering stage (TP-LHD) (Figure 3C). *CO-like* is an important regulator of photoperiodic response and flowering and was detected in clusters 9 and 15. *FT* genes, such as *HvFT1-1*, *HvFT1-2*, and *HvFT4*, also belonged to cluster 9 (Figure 3C). Previous studies have shown that *FT* acts downstream of CO and regulates flowering time.[69,70] Cluster 3 contained genes encoding an ARF, a TF that is specific to the seed-filling stage of the spike, and related to ABI3 and VP1 (RAV), a TF associated with response to ethylene and BRs[71] (Figure 3C).

Genes with different functions tend to exhibit substantially different expression profiles across developmental stages. We identified genes associated with GO terms involved in phytohormones, development, and metabolism in most stages (all 17 stages except GrA), and genes representing functionally similar GO terms were present in similar stages (Figure 4A; Table S6). We therefore attempted to correlate the possible role of genes with developmental stages. To this end, we performed a correlation analysis on the above genes and selected those with high correlations (Pearson's $r > 0.9$ or $r < -0.9$) to draw the resulting correlation network between known genes, phytohormone-related genes, and TF genes (Table S11). We detected a high correlation with cluster peak stage in the AP-YA window (clusters 1, 5, 6, 8, and 11), the TP-LHD period (clusters 2, 4, 7, 9, 13, 14, and 15), the 4–28 DFL period (cluster 3), and the 32–36 DFL window (clusters 12 and 10) (Figure 4B). This finding suggests that the expression pattern of barley genes is largely consistent with the dynamics of the major stages of the normal growth cycle. Using this correlation analysis, we can predict

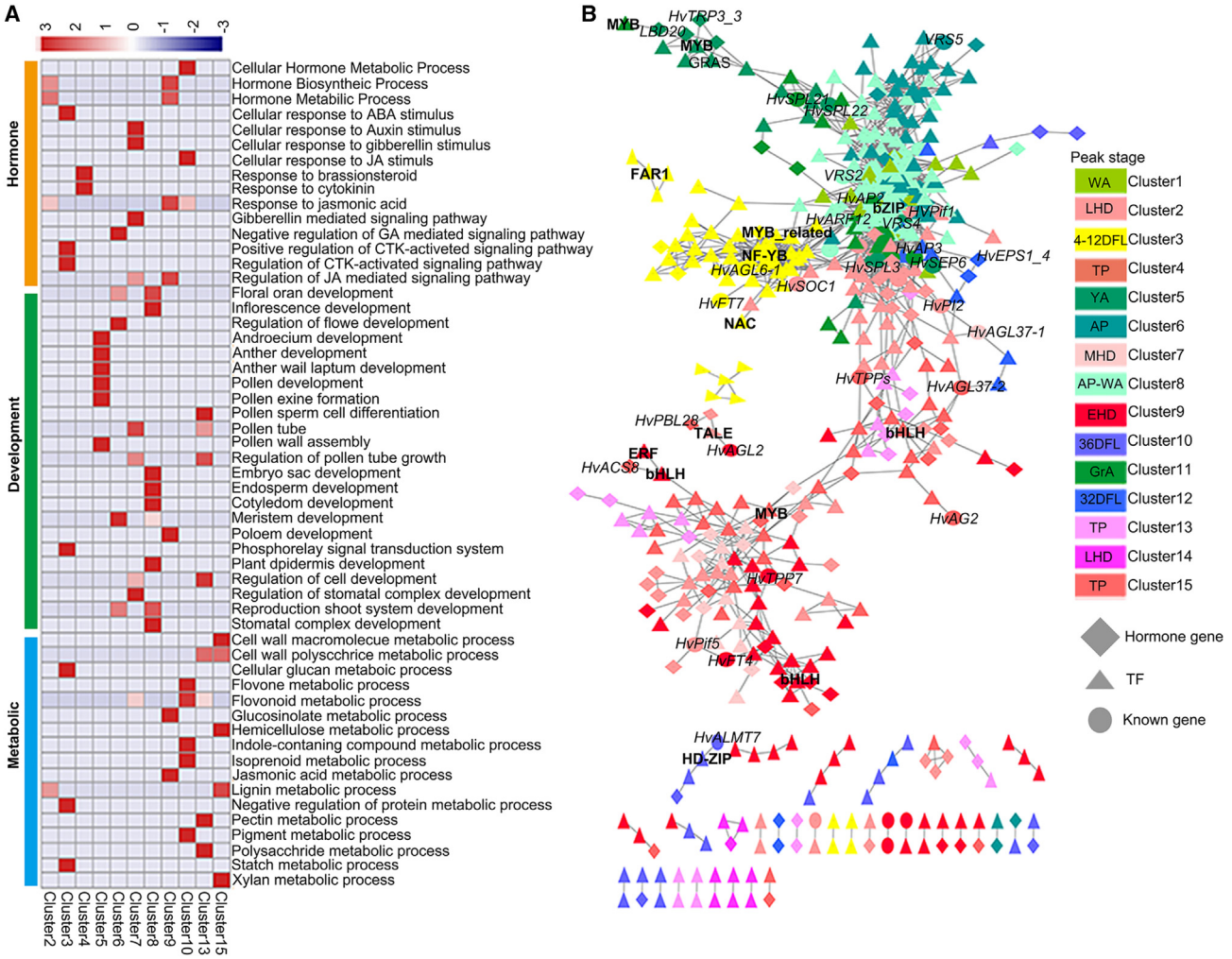

Figure 4. GO terms and networks of genes from different clusters

(A) Enriched GO terms (scaled −log10 [FDR-adjusted p value] > 1.30 and numerical normalization of rows) in the expression clusters identified in Figure 2C.

(B) Network of TF genes, phytohormone-related genes, and other known genes from different clusters (Pearson's coefficients > 0.95 or < –0.95). Different colors represent different clusters as indicated to the right. Diamonds represent phytohormone genes; triangles represent TF genes; and circles represent other known genes.

possible regulatory relationships among genes in different clusters. For example, although the expression patterns of *HvAGL6* and *HvSOC1* were specific to different clusters, they were highly correlated (Figure 4B; Table S11). Previous studies in Arabidopsis showed that *SOC1* expression is significantly upregulated in transgenic plants heterologously expressing *AGL6*.[72]

Network analysis identifies interrelated functional modules and important genes associated with spike length and spike weight

We applied weighted gene co-expression network analysis (WGCNA) to obtain a system-wide understanding of genes and TF genes whose co-expression patterns are highly correlated during spike development. Barley spike growth follows an S-growth curve, with a significant increase in spike length at the AP-LHD stage (Figure 5A). During post-anthesis, the main change in spike is an increase in spike weight traits (spike weight, lateral spikelet weight, central spikelet weight, and spikelet weight) (Figures 5B and 5C), reaching a maximum at 32 days after anthesis (Figure 5B). To identify the genes and TF genes that influence spike length and weight, we separated the 17 stages into 2 groups: spike length-increasing stages (AP-LHD) and spike weight-increasing stages (LHD–32 DFL); we then subjected each group to WGCNA.

We identified eight modules associated with spike length (Figure S2), and selected genes with linkage (linkage weight ≥ 0.3) within the module with a positive correlation in spike length (green, royal blue and dark green modules) (Table S12). We extracted TF genes and homologous genes for network analysis. In the network related to spike length, we noticed phytohormone-related genes and TF genes as potentially interacting to regulate spike length. The phytohormone-related genes included

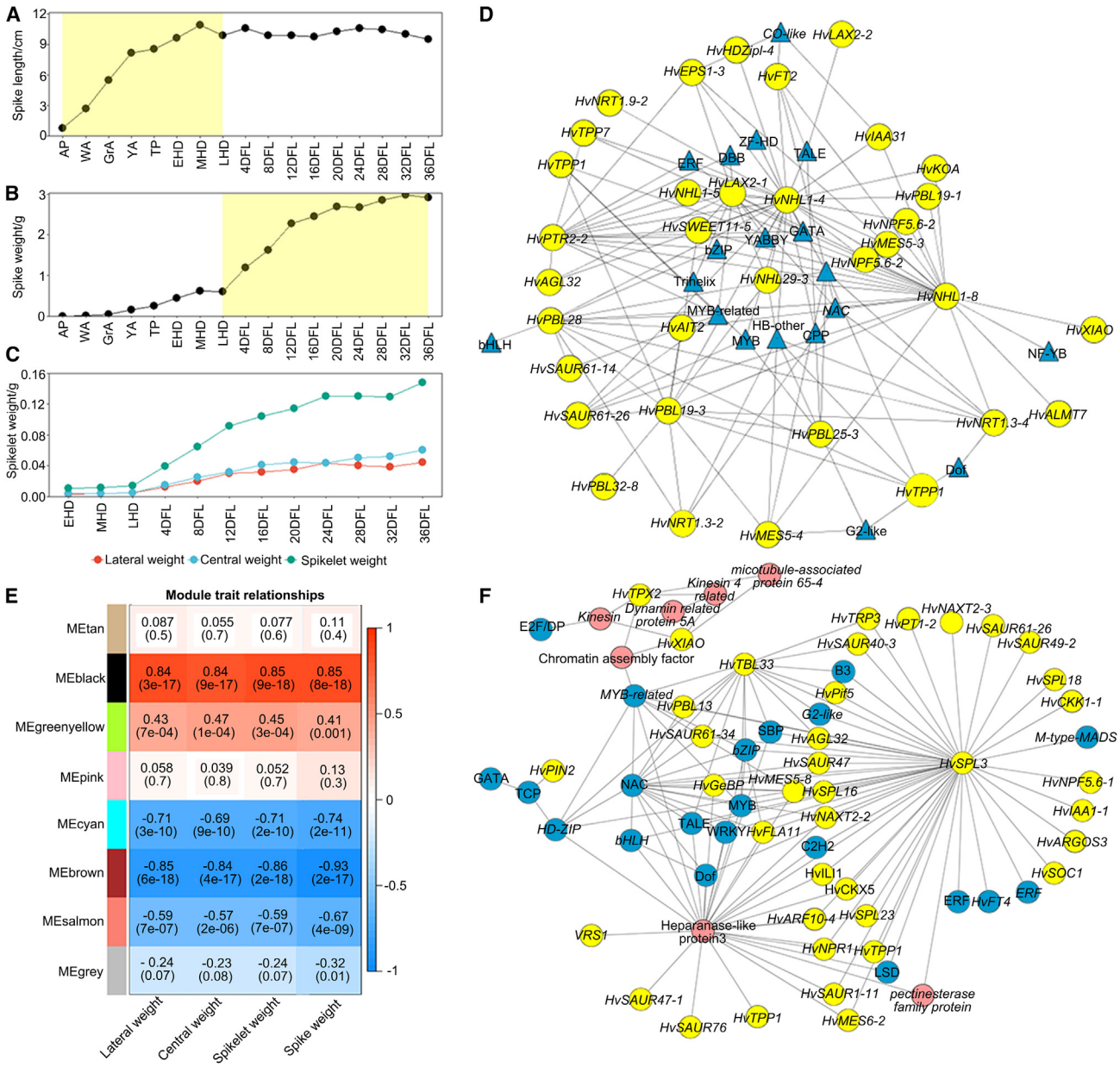

Figure 5. Network analysis identifies hub genes associated with spike length and weight

(A and B) Dynamics of spike length (A) and weight (B) across the 17 stages.

(C) Dynamics of lateral spikelet weight, central spikelet weight and the weight of the 3 spikelets at 1 rachis node (2 lateral spikelets and 1 central spikelet) across 12 stages following the early heading stage (EHD).

(D) Regulatory network of genes and TF genes for positive spike length-related modules. Blue triangles represent transcription factors and yellow circles indicate homologs or known published genes.

(E) Module trait relationship, numerical representation correlation; blue represents negative correlation, while red represents positive correlation.

(F) Regulatory network of genes and TF genes from the brown module. Blue circles represent transcription factors, yellow circles indicate homologous or published genes, and red circles represent other transcription factor-related genes in the module.

auxin-related genes (*HvIAA31*, *HvSAUR61-14*, *HvSAUR61-26*, *LIKE AUX1 2-2* [*HvLAX2-2*]), salicylic acid-related genes (*HvNHL1-8*, *HvNHL1-4*, *HvEPS1-3*, *HvMES5-3*), GA-related genes (*HvPYR2-2*), and BR genes (*HvPBL19-3*, *HvPBL28*, *HvPBL32-8*). In addition, several *NDR1/HIN1-like* (*NHL*) genes (*HvNHL1-4*, *HvNHL1-5*, *HvNHL1-8*, *HvNHL29-3*) were associated with spike length (Figure 5D). *NHL* genes trigger plant defense in response to biotic stresses and seed germination under chilling stress through the ABA pathway.[73] GO terms analysis revealed that genes in the red module are enriched in categories involved in

the regulation of shoot system development and cytokinin-activated signaling pathways (Figure S2D; Table S13). These results not only make it possible to understand the chain of events underlying spike elongation during spike development, but also help to identify key factors regulating spike length.

The correlation obtained from the WGCNA analysis means that the trait is correlated with the taxonomic module; the eigenvalues of the module are correlated with the expression of the genes. This does not mean that spike length is directly correlated with gene transcription levels. The WGCNA of spike weight-related traits identified eight modules (Figure S3), with consistent correlations between the different traits and the module (Figure 5E). We performed GO analyses on each of the eight modules and determined that genes in the black module are enriched in GO terms related to response to 1-aminocyclopropane-1-carboxylic acid, a precursor for the biosynthesis of the phytohormone ethylene[74] (Figure S3C), seed dormancy, seed maturation, protein stabilization, anatomical structure maturation, and developmental maturation (Table S14). Genes in the brown module were enriched in pathways related to the mitotic cell cycle and plant-type secondary cell wall biogenesis (Figure S3D). Notably, some important genes that are essential for floral development (e.g., *HvSPL13*, *HvSPL16*, *HvSPL18*, *HvSPL23*, *NAC*, *bHLH*, *bZIP*, *MYB*, *TCP*, *C2HC*, *B3*, *ERF*) were present in the brown module (Figure 5F). Genes in the brown module maintained their expression levels until the LHD stage (Table S14).

GDSL esterase/lipase genes in cluster 5 affect spike morphology

To verify the correlation between different gene expression patterns and their functions, we next selected genes from cluster 5 for in-depth analysis. The expression of the genes in cluster 5 peaked at YA stage (Figure 2C). This stage is an important period of spike development, during which pollen matures and prepares for the fertilization process. A large number of GO terms related to pollen, floral, and anther development were detected in cluster 5 (Table S6). Ten GDSL esterase/lipase protein genes were identified. GDSL esterase/lipase proteins are associated with pollen development and fertility in rice.[75,76] A GDSL esterase/lipase (GELP) gene (HORVU5Hr1G068460), orthologous to *OsGELP96* (http://plants.ensembl.org/index.html), had the highest expression level among these 10 genes (Figure S4). We named this gene *HvGELP96*. To investigate the function of this gene, we obtained a mutant in this gene from an ethyl methanesulfonate (EMS)-mutagenized population library[77] and derived homozygotes from the mutant line M7963, harboring an A203V substitution of HvGELP96. Compared with the wild-type "Hatiexi" (HTX), the homozygous mutant showed a reduction in spikelet fertility (Figures 6A and 6B) and significantly shorter and lighter spikes, together with fewer grains (Figures 6C–6E). The phenotypes of the mutant indicated that *HvGELP96* is associated with spike morphology in barley. Further functional verification of *HvGELP96* should be performed in the future.

DISCUSSION

To better understand the regulation of spikelet development in barley, we generated an RNA-seq dataset to spatially and temporally dissect gene expression over 17 stages and at 5 spikelet positions. High-quality barley reference genome was released in 2017.[8] Few studies about barley transcriptome have been reported.[78–81] Recently, using laser capture microdissected tissues, Thiel et al.[80] reported transcriptional landscapes of floral meristems in a two-rowed barley cultivar (Bowman). Compared with previous transcriptome work in barley, the samples in this study cover a longer window of spike development, and include the development of structures in five positions across individual spikes, providing a comprehensive analysis of gene expression patterns for spikelet development. We selected the six-rowed barley cultivar Morex because this variety eliminates the interference caused by the lack of lateral spikelets. In addition, complete genome sequencing data are available for Morex. Using these expression profile data, we summarized key features of gene expression related to spike development in barley.

Genes expressed at different stages display obvious different expression pattern

From the transcriptome data, we determined that the number of expressed genes gradually increases from the AP to the TP stages (Figure 1D). This window represents the development and maturation of stamens and pistils after spikelet primordium differentiation, and the completion of meiosis. The AP to TP stages, which are the most critical period for spikelet maximum survival yield potential in barley, are precisely regulated.[3] During these stages, genes involved in stamen development, meiosis, glucose transport, cell cycle, vascular bundle transport, and cell wall assembly are highly expressed, a result consistent with the development taking place during these stages (Figure 2D). During the TP-LHD stages (the early stage of carpel development), expression of a number of genes reached a peak (Figure 1D). The genes in pathways related to phytohormones such as cytokinins and JA and related to pollen tube elongation were highly expressed at certain stages (Figure 2D), suggesting that these phytohormone pathways are crucial for the regulation of carpel and pollen development. After LHD, the number of expressed genes decreased significantly until 36 DFL (Figure 1D). This period represents the gradual maturation of embryos and grains, primarily involving the accumulation of assimilates via associated metabolic pathways. By clustering the expressed genes at the 17 stages, we successfully identified key regulators for a variety of events during spike development.

Genes expressed in the apical spikelet are significantly different from those expressed in other parts of the spike

Based on our gene expression dataset of spikelets, we noticed that the number of DEGs for the top part of the spikelet is the largest (Figure 2B), indicating that gene expression directing the development of the apical spikelet is different from that in other parts. In panicle development of monocots, the development of the apical spikelet is regulated by specific genes, phytohormone levels, the environment, and other factors.[82] For example, previous studies largely focused on the regulation by auxin and cytokinins of the top of the spike.[60] In this study, we showed that expression of genes involved in the BR pathway

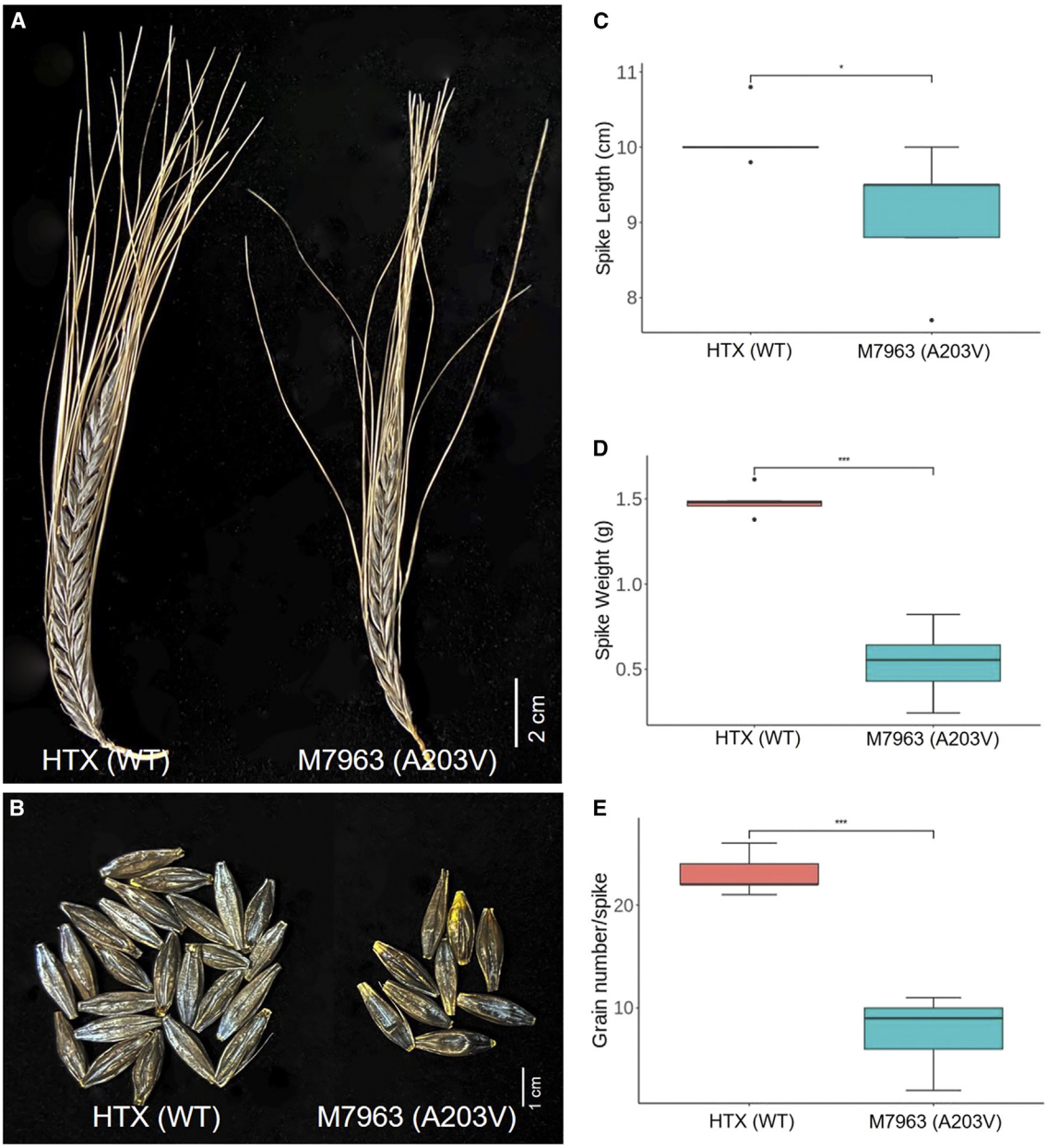

Figure 6. A GDSL esterase/lipase gene (HORVU5Hr1G068460, *HvGELP96*) affected spike morphology in barley

(A and B) Representative photograph of spikes (A) and grains of an individual spike (B) from the wild-type "Hatiexi" (HTX) and a homozygous M7963 mutant plant. (C–E) Spike length (C), spike weight (D), and grain number per spike (E) of the barley *gelp96* mutant and its wild-type (HTX). Data are means ± SD (n = 5 spikes). Significant differences were determined by Student's t test (*$p < 0.05$, ***$p < 0.001$).

is also higher in the apical spikelet, indicating that BR signaling contributes to the degradation and differentiation of the top of the spike. In rice, apical spikelets of rice panicles usually show degeneration characterized by small whitish spikelets with arrested development and sterile anthers, leading to failure of seed setting and a reduction in grain yield.[83,84] The development of the panicle apex is an important step that is closely related to yield. However, only a few genes associated with the degradation of apical spikelets have been identified to date, and the underlying mechanism at the top of the panicle needs to be explored further. In our expression profile data, over 1,000 genes were preferentially expressed in apical spikelets, offering a list of candidate genes for future analysis of the development and degeneration of apical spikelets.

The role of TFs in barley spike development

As important proteins regulating gene expression, TFs play crucial roles in spike development. For example, the TFs forming the ABC

model regulate the formation and morphological maintenance of lemmas, lodicules, stamens, and pistils. Four class E genes, *SEP1*, *SEP2*, *SEP3*, and *SEP4*, show partially redundant functions in determining the identity of sepals, petals, stamens, and carpels.[32,85] The genes *AGL6* and *AGL13* regulate floral organ formation, most likely in ovule formation.[86] In our RNA-seq data, the expression levels of *HvSEP5* and *HvSEP6* peaked at the GrA and YA stages, and their expression levels gradually decreased after the LHD stage (Figure 3A). This finding indicates that these two *SEP* genes also play an important regulatory role in the formation of floral organs during the GrA and YA stages. *SPL* genes have diverse functions, including roles in plant growth and development.[87,88] The expression patterns of *SPL* and *AGL* family genes were higher before LHD and then gradually decreased (Figure 3A), suggesting that their encoding TFs regulate inflorescence development mainly before flowering. Using our expression profile data, we can predict new functions for some previously well-known genes.

In summary, the high spatiotemporal resolution of our transcriptome dataset revealed a number of key regulators and fundamental regulatory networks for the development of spike tissues in barley. It will not only facilitate functional analysis of relevant genes and molecular patterns of spike development and morphology, but also provide information that is helpful, if not essential, for the improvement of grain yield during barley breeding.

Limitations of the study

The AP stage was the starting point for sample collection in this work. However, the developmental process before AP stage is also important, transcriptome analyses can be performed specifically for this developmental stage. In addition, we identified a series of genes associated with different developmental events, and only one gene was selected for function validation, more important genes can be investigated. We investigated the phenotypes of the candidate gene using EMS mutants, and the results would be better if there were knockout mutants and overexpressed lines.

STAR★METHODS

Detailed methods are provided in the online version of this paper and include the following:

- KEY RESOURCES TABLE
- RESOURCE AVAILABILITY
  - Lead contact
  - Materials availability
  - Data and code availability
- EXPERIMENTAL MODEL AND SUBJECT DETAILS
  - Plant materials and growth conditions
- METHOD DETAILS
  - Sample collection for transcriptome analysis
  - Tissue preparation and mRNA sequencing
  - Read mapping and differential gene expression analysis
  - Differentially expressed genes (DEGs) throughout the reproductive period (AP-36DFL)
  - Differential expression of genes in the top, middle and bottom positions during the same developmental stage
  - Clustering of gene expression profiles and GO enrichment analysis
  - Weighted gene co-expression network analysis (WGCNA)
  - Mutant identification
- QUANTIFICATION AND STATISTICAL ANALYSIS

SUPPLEMENTAL INFORMATION

Supplemental information can be found online at https://doi.org/10.1016/j.celrep.2023.113441.

ACKNOWLEDGMENTS

We thank Thorsten Schnurbusch (Leibniz Institute of Plant Genetics and Crop Plant Research, IPK) and IPK for providing greenhouse space for the collections of transcriptome samples. We thank Dongdong Xu (Institute of Industrial Crops, Shandong Academy of Agricultural Sciences, Jinan, 250100, China) for help on bioinformatics analysis.

AUTHOR CONTRIBUTIONS

Z.G. conceived the project and supervised the experiments. L.S. conducted the mutant genotypic identification and spike phenotype measurement. Y.L. and Y.J. performed data analyses. Y.L., L.S., Z.W., Z.S., L.Z., and K.S. measured the spike morphology traits. Z.G., L.S., and Y.L. wrote the manuscript. All the authors viewed and edited the manuscript.

DECLARATION OF INTERESTS

The authors declare no competing interests.

Received: January 10, 2022
Revised: July 6, 2023
Accepted: October 31, 2023

REFERENCES

1. Zohary, D., and Hopf, M. (2000). Domestication of Plants in the Old World : The Origin and Spread of Cultivated Plants in West Asia, Europe and the Nile Valley (No. Ed. 3) (Oxford university press).
2. Helback, H. (1959). Domestication of Food Plants in the Old World: Joint efforts by botanists and archeologists illuminate the obscure history of plant domestication. Science *130*, 365–372.
3. Alqudah, A.M., and Schnurbusch, T. (2014). Awn primordium to tipping is the most decisive developmental phase for spikelet survival in barley. Funct. Plant Biol. *41*, 424–436.
4. Sreenivasulu, N., and Schnurbusch, T. (2012). A genetic playground for enhancing grain number in cereals. Trends Plant Sci. *17*, 91–101.
5. Sebastián, A., Miralles, D.J., and Miralles. (2006). Floret development and grain setting in near isogenic two- and six-rowed barley lines (Hordeum vulgare L.). Field Crop Res *96*, 466–476.
6. Boussora, F., Allam, M., Guasmi, F., Ferchichi, A., Rutten, T., Hansson, M., Youssef, H.M., and Börner, A. (2019). Spike developmental stages and ABA role in spikelet primordia abortion contribute to the final yield in barley (Hordeum vulgare L.). Bot. Stud. *60*, 13.
7. International Barley Genome Sequencing Consortium; Mayer, K.F.X., Waugh, R., Brown, J.W.S., Schulman, A., Langridge, P., Platzer, M., Fincher, G.B., Muehlbauer, G.J., Sato, K., et al. (2012). A physical, genetic

and functional sequence assembly of the barley genome. Nature *491*, 711–716.

8. Mascher, M., Gundlach, H., Himmelbach, A., Beier, S., Twardziok, S.O., Wicker, T., Radchuk, V., Dockter, C., Hedley, P.E., Russell, J., et al. (2017). A chromosome conformation capture ordered sequence of the barley genome. Nature *544*, 427–433.
9. Kirby, E.J.M., and Appleyard, M. (1987). Development and structure of the wheat plant. Wheat Breeding, 287–311.
10. Waddington, S.R., Cartwright, P.M., and Wall, P.C. (1983). A Quantitative Scale of Spike Initial and Pistil Development in Barley and Wheat. Ann. Bot. *51*, 119–130.
11. Kirby, E., and Appleyard, M. (1984). Cereal development guide. 2nd Edition.
12. Futschik, M.E., and Carlisle, B. (2005). Noise-robust soft clustering of gene expression time-course data. J. Bioinform. Comput. Biol. *3*, 965–988.
13. Bomblies, K., Wang, R.L., Ambrose, B.A., Schmidt, R.J., Meeley, R.B., and Doebley, J. (2003). Duplicate FLORICAULA/LEAFY homologs zfl1 and zfl2 control inflorescence architecture and flower patterning in maize. Development *130*, 2385–2395.
14. Ye, B.B., Shang, G.D., Pan, Y., Xu, Z.G., Zhou, C.M., Mao, Y.B., Bao, N., Sun, L., Xu, T., and Wang, J.W. (2020). AP2/ERF Transcription Factors Integrate Age and Wound Signals for Root Regeneration. Plant Cell *32*, 226–241.
15. Romanova, M.A., Maksimova, A.I., Pawlowski, K., and Voitsekhovskaja, O.V. (2021). YABBY Genes in the Development and Evolution of Land Plants. Int. J. Mol. Sci. *22*, 4139.
16. Nonomura, K.I., Nakano, M., Fukuda, T., Eiguchi, M., Miyao, A., Hirochika, H., and Kurata, N. (2004). The novel gene HOMOLOGOUS PAIRING ABERRATION IN RICE MEIOSIS1 of rice encodes a putative coiled-coil protein required for homologous chromosome pairing in meiosis. Plant Cell *16*, 1008–1020.
17. Fukuda, T., Daniel, K., Wojtasz, L., Toth, A., and Höög, C. (2010). A novel mammalian HORMA domain-containing protein, HORMAD1, preferentially associates with unsynapsed meiotic chromosomes. Exp. Cell Res. *316*, 158–171.
18. Hu, Y., Wang, L., Jia, R., Liang, W., Zhang, X., Xu, J., Chen, X., Lu, D., Chen, M., Luo, Z., et al. (2021). Rice transcription factor MADS32 regulates floral patterning through interactions with multiple floral homeotic genes. J. Exp. Bot. *72*, 2434–2449.
19. Sun, Q., Qu, J., Yu, Y., Yang, Z., Wei, S., Wu, Y., Yang, J., and Peng, Z. (2019). TaEPFL1, an EPIDERMAL PATTERNING FACTOR-LIKE (EPFL) secreted peptide gene, is required for stamen development in wheat. Genetica *147*, 121–130.
20. Wang, H., and Wang, H. (2015). The miR156/SPL Module, a Regulatory Hub and Versatile Toolbox, Gears up Crops for Enhanced Agronomic Traits. Mol. Plant *8*, 677–688.
21. Unte, U.S., Sorensen, A.M., Pesaresi, P., Gandikota, M., Leister, D., Saedler, H., and Huijser, P. (2003). SPL8, an SBP-box gene that affects pollen sac development in Arabidopsis. Plant Cell *15*, 1009–1019.
22. Jack, T., Brockman, L.L., and Meyerowitz, E.M. (1992). The homeotic gene APETALA3 of Arabidopsis thaliana encodes a MADS box and is expressed in petals and stamens. Cell *68*, 683–697.
23. Riechmann, J.L., Krizek, B.A., and Meyerowitz, E.M. (1996). Dimerization specificity of Arabidopsis MADS domain homeotic proteins APETALA1, APETALA3, PISTILLATA, and AGAMOUS. Proc. Natl. Acad. Sci. USA *93*, 4793–4798.
24. Jack, T. (2001). Relearning our ABCs: new twists on an old model. Trends Plant Sci. *6*, 310–316.
25. Li, G., Kuijer, H.N.J., Yang, X., Liu, H., Shen, C., Shi, J., Betts, N., Tucker, M.R., Liang, W., Waugh, R., et al. (2021). MADS1 maintains barley spike morphology at high ambient temperatures. Nat. Plants *7*, 1093–1107.
26. Debernardi, J.M., Greenwood, J.R., Jean Finnegan, E., Jernstedt, J., and Dubcovsky, J. (2020). APETALA 2-like genes AP2L2 and Q specify lemma identity and axillary floral meristem development in wheat. Plant J. *101*, 171–187.
27. Zadoks, J.C., Chang, T.T., and Konzak, C.F. (1974). A decimal code for growth stages of cereals. Weed Res. *14*, 415–421.
28. Faure, S., Higgins, J., Turner, A., and Laurie, D.A. (2007). The FLOWERING LOCUS T-like gene family in barley (Hordeum vulgare). Genetics *176*, 599–609.
29. Pieper, R., Tomé, F., Pankin, A., and von Korff, M. (2021). FLOWERING LOCUS T4 delays flowering and decreases floret fertility in barley. J. Exp. Bot. *72*, 107–121.
30. Bi, X., van Esse, W., Mulki, M.A., Kirschner, G., Zhong, J., Simon, R., and von Korff, M. (2019). CENTRORADIALIS Interacts with FLOWERING LOCUS T-Like Genes to Control Floret Development and Grain Number. Plant Physiol. *180*, 1013–1030.
31. Bowman, J.L., Smyth, D.R., and Meyerowitz, E.M. (1989). Genes directing flower development in Arabidopsis. Plant Cell *1*, 37–52.
32. Ditta, G., Pinyopich, A., Robles, P., Pelaz, S., and Yanofsky, M.F. (2004). The SEP4 gene of Arabidopsis thaliana functions in floral organ and meristem identity. Curr. Biol. *14*, 1935–1940.
33. Flanagan, C.A., and Ma, H. (1994). Spatially and temporally regulated expression of the MADS-box gene AGL2 in wild-type and mutant arabidopsis flowers. Plant Mol. Biol. *26*, 581–595.
34. Lee, J., and Lee, I. (2010). Regulation and function of SOC1, a flowering pathway integrator. J. Exp. Bot. *61*, 2247–2254.
35. Lin, Q., Wang, S., Dao, Y., Wang, J., and Wang, K. (2020). Arabidopsis thaliana trehalose-6-phosphate phosphatase gene TPPI enhances drought tolerance by regulating stomatal apertures. J. Exp. Bot. *71*, 4285–4297.
36. Kretzschmar, T., Pelayo, M.A.F., Trijatmiko, K.R., Gabunada, L.F.M., Alam, R., Jimenez, R., Mendioro, M.S., Slamet-Loedin, I.H., Sreenivasulu, N., Bailey-Serres, J., et al. (2015). A trehalose-6-phosphate phosphatase enhances anaerobic germination tolerance in rice. Nat. Plants *1*, 15124.
37. Li, Y., Xiong, H., Cuo, D., Wu, X., and Duan, R. (2019). Genome-wide characterization and expression profiling of the relation of the HD-Zip gene family to abiotic stress in barley (Hordeum vulgare L.). Plant Physiol. Biochem. *141*, 250–258.
38. Baroja-Fernández, E., Muñoz, F.J., Li, J., Bahaji, A., Almagro, G., Montero, M., Etxeberria, E., Hidalgo, M., Sesma, M.T., and Pozueta-Romero, J. (2012). Sucrose synthase activity in the sus1/sus2/sus3/sus4 Arabidopsis mutant is sufficient to support normal cellulose and starch production. Proc. Natl. Acad. Sci. USA *109*, 321–326.
39. Deng, Y., Wang, J., Zhang, Z., and Wu, Y. (2020). Transactivation of Sus1 and Sus2 by Opaque2 is an essential supplement to sucrose synthase-mediated endosperm filling in maize. Plant Biotechnol. J. *18*, 1897–1907.
40. Hou, J., Jiang, Q., Hao, C., Wang, Y., Zhang, H., and Zhang, X. (2014). Global selection on sucrose synthase haplotypes during a century of wheat breeding. Plant Physiol. *164*, 1918–1929.
41. Tao, J., Liang, W., An, G., and Zhang, D. (2018). OsMADS6 Controls Flower Development by Activating Rice FACTOR OF DNA METHYLATION LIKE1. Plant Physiol. *177*, 713–727.
42. Su, Y., Liu, J., Liang, W., Dou, Y., Fu, R., Li, W., Feng, C., Gao, C., Zhang, D., Kang, Z., and Li, H. (2019). Wheat AGAMOUS LIKE 6 transcription factors function in stamen development by regulating the expression of Ta APETALA3. Development *146*, dev177527.
43. Rawlings, N.D., Tolle, D.P., and Barrett, A.J. (2004). Evolutionary families of peptidase inhibitors. Biochem. J. *378*, 705–716.
44. Zhang, P., Wang, F., Zhang, L.F., Rui, Q., and Xu, L.L. (2006). The role of serine endopeptidase in cucumber leaf senescence. Zhi Wu Sheng Li Yu Fen Zi Sheng Wu Xue Xue Bao *32*, 593–599.
45. Li, C.Y., Li, W.H., Li, C., Gaudet, D.A., Laroche, A., Cao, L.P., and Lu, Z.X. (2010). Starch synthesis and programmed cell death during endosperm development in triticale (x Triticosecale Wittmack). J. Integr. Plant Biol. *52*, 602–615.

46. Young, T.E., and Gallie, D.R. (2000). Programmed cell death during endosperm development. Plant Mol. Biol. *44*, 283–301.

47. Hong-Bo, S., Zong-Suo, L., and Ming-An, S. (2005). LEA proteins in higher plants: structure, function, gene expression and regulation. Colloids Surf. B Biointerfaces *45*, 131–135.

48. Tiwari, S.B., Hagen, G., and Guilfoyle, T. (2003). The roles of auxin response factor domains in auxin-responsive transcription. Plant Cell *15*, 533–543.

49. Truskina, J., Han, J., Chrysanthou, E., Galvan-Ampudia, C.S., Lainé, S., Brunoud, G., Macé, J., Bellows, S., Legrand, J., Bågman, A.M., et al. (2021). A network of transcriptional repressors modulates auxin responses. Nature *589*, 116–119.

50. Hayashi, K.I., Arai, K., Aoi, Y., Tanaka, Y., Hira, H., Guo, R., Hu, Y., Ge, C., Zhao, Y., Kasahara, H., and Fukui, K. (2021). The main oxidative inactivation pathway of the plant hormone auxin. Nat. Commun. *12*, 6752.

51. Wei, Z., and Li, J. (2016). Brassinosteroids Regulate Root Growth, Development, and Symbiosis. Mol. Plant *9*, 86–100.

52. Shi, H., Li, X., Lv, M., and Li, J. (2022). BES1/BZR1 Family Transcription Factors Regulate Plant Development via Brassinosteroid-Dependent and Independent Pathways. Int. J. Mol. Sci. *23*, 10149.

53. Lin, W.H. (2020). Designed Manipulation of the Brassinosteroid Signal to Enhance Crop Yield. Front. Plant Sci. *11*, 854.

54. Majer, C., and Hochholdinger, F. (2011). Defining the boundaries: structure and function of LOB domain proteins. Trends Plant Sci. *16*, 47–52.

55. Xu, C., Luo, F., and Hochholdinger, F. (2016). LOB Domain Proteins: Beyond Lateral Organ Boundaries. Trends Plant Sci. *21*, 159–167.

56. Corratgé-Faillie, C., and Lacombe, B. (2017). Substrate (un)specificity of Arabidopsis NRT1/PTR FAMILY (NPF) proteins. J. Exp. Bot. *68*, 3107–3113.

57. Ren, H., and Gray, W.M. (2015). SAUR Proteins as Effectors of Hormonal and Environmental Signals in Plant Growth. Mol. Plant *8*, 1153–1164.

58. Kurepin, L.V., Dahal, K.P., Savitch, L.V., Singh, J., Bode, R., Ivanov, A.G., Hurry, V., and Hüner, N.P.A. (2013). Role of CBFs as Integrators of Chloroplast Redox, Phytochrome and Plant Hormone Signaling during Cold Acclimation. Int. J. Mol. Sci. *14*, 12729–12763.

59. Mravec, J., Skůpa, P., Bailly, A., Hoyerová, K., Krecek, P., Bielach, A., Petrásek, J., Zhang, J., Gaykova, V., Stierhof, Y.D., et al. (2009). Subcellular homeostasis of phytohormone auxin is mediated by the ER-localized PIN5 transporter. Nature *459*, 1136–1140.

60. Youssef, H.M., and Hansson, M. (2019). Crosstalk among hormones in barley spike contributes to the yield. Plant Cell Rep. *38*, 1013–1016.

61. Zhang, T., Li, C., Li, D., Liu, Y., and Yang, X. (2020). Roles of YABBY transcription factors in the modulation of morphogenesis, development, and phytohormone and stress responses in plants. J. Plant Res. *133*, 751–763.

62. Sun, L., Wei, Y.Q., Wu, K.H., Yan, J.Y., Xu, J.N., Wu, Y.R., Li, G.X., Xu, J.M., Harberd, N.P., Ding, Z.J., and Zheng, S.J. (2021). Restriction of Iron Loading into Developing Seeds by A YABBY Transcription Factor Safeguards Successful Reproduction in Arabidopsis. Mol. Plant *14*, 1624–1639.

63. Lai, X., Blanc-Mathieu, R., GrandVuillemin, L., Huang, Y., Stigliani, A., Lucas, J., Thévenon, E., Loue-Manifel, J., Turchi, L., Daher, H., et al. (2021). The LEAFY floral regulator displays pioneer transcription factor properties. Mol. Plant *14*, 829–837.

64. Jin, R., Klasfeld, S., Zhu, Y., Fernandez Garcia, M., Xiao, J., Han, S.K., Konkol, A., and Wagner, D. (2021). LEAFY is a pioneer transcription factor and licenses cell reprogramming to floral fate. Nat. Commun. *12*, 626.

65. Horiguchi, G., Kim, G.T., and Tsukaya, H. (2005). The transcription factor AtGRF5 and the transcription coactivator AN3 regulate cell proliferation in leaf primordia of Arabidopsis thaliana. Plant J. *43*, 68–78.

66. Kim, J.H., Choi, D., and Kende, H. (2003). The AtGRF family of putative transcription factors is involved in leaf and cotyledon growth in Arabidopsis. Plant J. *36*, 94–104.

67. Kim, J.H., and Kende, H. (2004). A transcriptional coactivator, AtGIF1, is involved in regulating leaf growth and morphology in Arabidopsis. Proc. Natl. Acad. Sci. USA *101*, 13374–13379.

68. Lee, B.H., Ko, J.H., Lee, S., Lee, Y., Pak, J.H., and Kim, J.H. (2009). The Arabidopsis GRF-INTERACTING FACTOR Gene Family Performs an Overlapping Function in Determining Organ Size as Well as Multiple Developmental Properties. Plant Physiol. *151*, 655–668.

69. Yang, T., He, Y., Niu, S., Yan, S., and Zhang, Y. (2020). Identification and characterization of the CONSTANS (CO)/CONSTANS-like (COL) genes related to photoperiodic signaling and flowering in tomato. Plant Sci. *301*, 110653.

70. Putterill, J., Laurie, R., and Macknight, R. (2004). It's time to flower: the genetic control of flowering time. Bioessays *26*, 363–373.

71. Nakano, T., Suzuki, K., Fujimura, T., and Shinshi, H. (2006). Genome-wide analysis of the ERF gene family in Arabidopsis and rice. Plant Physiol. *140*, 411–432.

72. Fan, J., Li, W., Dong, X., Guo, W., and Shu, H. (2007). Ectopic expression of a hyacinth AGL6 homolog caused earlier flowering and homeotic conversion in Arabidopsis. Sci. China C Life Sci. *50*, 676–689.

73. Wang, J., Wu, R., Shangguan, T., Chen, G., Zheng, Y., Tao, X., Li, S., Wang, Y., and Xu, S. (2022). NDR1/HIN1-like genes may regulate Glycine max seed germination under chilling stress through the ABA pathway. Plant Growth Regul. *98*, 613–624.

74. Barry, C.S., Llop-Tous, M.I., and Grierson, D. (2000). The Regulation of 1-Aminocyclopropane-1-Carboxylic Acid Synthase Gene Expression during the Transition from System-1 to System-2 Ethylene Synthesis in Tomato 1. Plant Physiol. *123*, 979–986.

75. Zhao, J., Long, T., Wang, Y., Tong, X., Tang, J., Li, J., Wang, H., Tang, L., Li, Z., Shu, Y., et al. (2020). RMS2 Encoding a GDSL Lipase Mediates Lipid Homeostasis in Anthers to Determine Rice Male Fertility. Plant Physiol. *182*, 2047–2064.

76. Zhang, H., Wang, M., Li, Y., Yan, W., Chang, Z., Ni, H., Chen, Z., Wu, J., Xu, C., Deng, X.W., and Tang, X. (2020). GDSL esterase/lipases OsGELP34 and OsGELP110/OsGELP115 are essential for rice pollen development. J. Integr. Plant Biol. *62*, 1574–1593.

77. Jiang, C., Lei, M., Guo, Y., Gao, G., Shi, L., Jin, Y., Cai, Y., Himmelbach, A., Zhou, S., He, Q., et al. (2022). A reference-guided TILLING by amplicon-sequencing platform supports forward and reverse genetics in barley. Plant Commun. *3*, 100317.

78. Arlt, C., Wachtmeister, T., Köhrer, K., and Stich, B. (2023). Affordable, accurate and unbiased RNA sequencing by manual library miniaturization: A case study in barley. Plant Biotechnol. J. *21*, 2241–2253.

79. Bhattacharyya, S., Giridhar, M., Meier, B., Peiter, E., Vothknecht, U.C., and Chigri, F. (2023). Global transcriptome profiling reveals root-and leaf-specific responses of barley (Hordeum vulgare L.) to H_2O_2. Front. Plant Sci. *14*, 1223778.

80. Thiel, J., Koppolu, R., Trautewig, C., Hertig, C., Kale, S.M., Erbe, S., Mascher, M., Himmelbach, A., Rutten, T., Esteban, E., et al. (2021). Transcriptional landscapes of floral meristems in barley. Sci. Adv. *7*, eabf0832.

81. Chen, G., Mishina, K., Wang, Q., Zhu, H., Tagiri, A., Kikuchi, S., Sassa, H., Oono, Y., and Komatsuda, T. (2023). Organ-enriched gene expression during floral morphogenesis in wild barley. Plant J. *116*, 887–902.

82. Xing, Y., and Zhang, Q. (2010). Genetic and molecular bases of rice yield. Annu. Rev. Plant Biol. *61*, 421–442.

83. Bai, J., Dong, G., Zhu, L., Zheng, H., Xie, Q., Nian, J., Ba, X., Zhu, X., Wang, Q., Zhang, J., and Chen, H. (2015). RiceTUTOU1Encodes a Suppressor of cAMP Receptor-Like Protein That Is Important for Actin Organization and Panicle Development. Plant Physiol. *169*, 1179–1191.

84. Jiang, S., Wang, J., Liu, D., Chen, L., Zhang, X., Xu, F., Sun, S., Jiang, H., Ding, G., Wang, T., et al. (2016). Mapping and candidate gene analysis for a new top spikelet abortion mutant in rice. Plant Breed. *135*, 155–165.

85. Pelaz, S., Ditta, G.S., Baumann, E., Wisman, E., and Yanofsky, M.F. (2000). B and C floral organ identity functions requireSEPALLATAMADS-box genes. Nature *405*, 200–203.

86. Schauer, S.E., Schlüter, P.M., Baskar, R., Gheyselinck, J., Bolaños, A., Curtis, M.D., and Grossniklaus, U. (2009). Intronic regulatory elements determine the divergent expression patterns of AGAMOUS-LIKE6 subfamily members in Arabidopsis. Plant J. *59*, 987–1000.

87. Chen, X., Zhang, Z., Liu, D., Zhang, K., Li, A., and Mao, L. (2010). SQUAMOSA promoter-binding protein-like transcription factors: star players for plant growth and development. J. Integr. Plant Biol. *52*, 946–951.

88. Wang, J.W. (2014). Regulation of flowering time by the miR156-mediated age pathway. J. Exp. Bot. *65*, 4723–4730.

89. Andrews, S. (2010). FastQC: a quality control tool for high throughput sequence Data.

90. Bolger, A.M., Lohse, M., and Usadel, B. (2014). Trimmomatic: a flexible trimmer for Illumina sequence data. Bioinformatics *30*, 2114–2120.

91. Patro, R., Duggal, G., Love, M.I., Irizarry, R.A., and Kingsford, C. (2017). Salmon provides fast and bias-aware quantification of transcript expression. Nat. Methods *14*, 417–419.

92. Soneson, C., Love, M.I., and Robinson, M.D. (2015). Differential analyses for RNA-seq: transcript-level estimates improve gene-level inferences. F1000Res. *4*, 1521.

93. Fischer, D.S., Theis, F.J., and Yosef, N. (2018). Impulse model-based differential expression analysis of time course sequencing data. Nucleic Acids Res. *46*, e119.

94. Love, M.I., Huber, W., and Anders, S. (2014). Moderated estimation of fold change and dispersion for RNA-seq data with DESeq2. Genome Biol. *15*, 550.

95. Kumar, L., and E Futschik, M. (2007). Mfuzz: a software package for soft clustering of microarray data. Bioinformation *2*, 5–7.

96. Cantalapiedra, C.P., Hernández-Plaza, A., Letunic, I., Bork, P., and Huerta-Cepas, J. (2021). eggNOG-mapper v2: Functional Annotation, Orthology Assignments, and Domain Prediction at the Metagenomic Scale. Mol. Biol. Evol. *38*, 5825–5829.

97. Wu, T., Hu, E., Xu, S., Chen, M., Guo, P., Dai, Z., Feng, T., Zhou, L., Tang, W., Zhan, L., et al. (2021). clusterProfiler 4.0: A universal enrichment tool for interpreting omics data. Innovation *2*, 100141.

98. Langfelder, P., and Horvath, S. (2008). WGCNA: an R package for weighted correlation network analysis. BMC Bioinf. *9*, 559.

99. Shannon, P., Markiel, A., Ozier, O., Baliga, N.S., Wang, J.T., Ramage, D., Amin, N., Schwikowski, B., and Ideker, T. (2003). Cytoscape: a software environment for integrated models of biomolecular interaction networks. Genome Res. *13*, 2498–2504.

STAR★METHODS

KEY RESOURCES TABLE

REAGENT or RESOURCE	SOURCE	IDENTIFIER
Chemicals, peptides, and recombinant proteins		
TRIzol™ Reagent	Invitrogen	Cat# 15596018
DNase I	Promega	Cat# Z3585
Phanta Max Master Mix (Dye Plus)	Vazyme	P525-01
Critical commercial assays		
RNeasy Plant Mini Kit	QIAGEN	74904
Next Ultra™ RNA Library Prep Kit	NEB	E7530L
TruSeq PE Cluster Kit v3-cBot-HS	Illumina	PE-401-3001
Plant Genomic DNA Extraction Kit	Tiangen	DP305-03
Deposited data		
Raw data of RNA-sequencing	This paper	CRA011642
Experimental models: Organisms/strains		
Barley: Morex	This paper	N/A
Barley: hatiexi (HTX)	This paper	N/A
Barley: hvgelp96	Jiang et al.[77]	N/A
Oligonucleotides		
Forward PCR primer for mutant genotyping: 5′-GTGATGGTAGCAGCCATGGTA-3′	This paper	N/A
Reverse primer for mutant genotyping: 5′-TACCAAGACTCCGCTATGGC-3′	This paper	N/A
Software and algorithms		
Fastqc	Andrews.[89]	http://www.bioinformatics.babraham.ac.uk/projects/fastqc/
Trimmomatic	Bolger et al.[90]	http://www.usadellab.org/cms/index.php?page=trimmomatic
Salmon	Patro et al.[91]	https://combine-lab.github.io/salmon/
Tximport package	Soneson et al.[92]	https://github.com/mikelove/tximport
ImpulseDE2 (v1.6.1)	Fischer et al.[93]	https://github.com/YosefLab/ImpulseDE2
DESeq2	Love et al.[94]	https://bioconductor.org/packages/release/bioc/html/DESeq2.html
Mfuzz package	Kumar et al.[95]	http://mfuzz.sysbiolab.eu/
Eggnog Mapper	Cantalapiedra et al.[96]	http://eggnog-mapper.embl.de
ClusterProfiler	Wu et al.[97]	http://bioconductor.org/packages/release/bioc/html/clusterProfiler.html
WGCNA package	Langfelder et al.[98]	http://www.genetics.ucla.edu/labs/horvath/CoexpressionNetwork/
Cytoscape3.7.1	Shannon et al.[99]	http://cytoscape.org

RESOURCE AVAILABILITY

Lead contact

Further information and requests for resources should be directed to the Lead contact, Zifeng Guo (guozifeng@ibcas.ac.cn).

Materials availability

Plant materials generated in this study are available from the lead contact on request.

This study did not generate new unique reagents.

Data and code availability

- The raw sequence data reported in this paper have been deposited in National Genomics Data Center (https://ngdc.cncb.ac.cn/gsa) under accession number CRA011642.
- This paper does not report original code.
- Any additional information required to reanalyze the data reported in this paper is available from the lead contact upon request.

EXPERIMENTAL MODEL AND SUBJECT DETAILS

Plant materials and growth conditions

Six-rowed barley (*Hordeum vulgare* cv. Morex) plants, wild-type "Hatiexi" (HTX) and *the mutant of HvGELP96* (*gelp96*) were grown in a greenhouse under the photoperiod of 16-h light/8-h dark, temperature of ~20°C day/~16°C night and light intensity of 250 μmol m^{-2} s^{-1}. Seeds were germinated in Petri dishes with water-soaked paper for 4 days. Four seedlings were transplanted to one pot (19 × 19 × 18 cm, 6.5 L). Supplemental light was supplied and plants were irrigated when required.

METHOD DETAILS

Sample collection for transcriptome analysis

Spikes were manually dissected for an overall view of floret development and abortion at 17 spikelet developmental stages in barley: 1) the awn primordium (AP) stage (the spikelet primordium number reaches its maximum); 2) the white anther (WA) stage (the anthers are partially surrounded by the young carpel, the two bumps at the top of the carpel initiate the development of styles and stigma, the palea partially encloses the carpel and stamen, the rachilla can be seed between the palea and lemma); 3) the green anther (GrA) stage (the stamens grow to approximately 1 mm in length, the carpel is enclosed by the lemma and palea); 4) the yellow anther (YA) stage (development of the anthers and pollen is more advanced, the lemma and palea grow and completely enclose the stamens and carpel); 5) the tipping (TP) stage (the tips of awns are visible); 6) the early heading (EHD) stage (the tip of the top spikelet is visible); 7) the middle heading (MHD) stage (half of the spike is visible); 8) the late heading (LHD) stages (more that 90% of the spike is visible). (9–17) Days following late heading. Information describing these different developmental stages can be found elsewhere.[9,11,27]

For the temporal transcriptome analysis of the six-rowed cultivar Morex, spikelets we harvested at each rachis node at each of the 17 developmental stages (Figure 1). For the spatial transcriptome analysis of spikelet gene expression, all three spikelets were used at each rachis node at each of the five positions of the rachis node (Figure 1) within each individual spike. Three biological replicates were collected for each of the time points/positions. Each replicate was obtained by pooling samples from at least five to ten plants. Total RNA was extracted using TRIzol reagent (Invitrogen).

At all 17 spike developmental stages, spike length and spike dry weight were measured. At 14 stages (excluding the AP, GrA, and YA stages) and the five positions, awn dry weight, spikelet dry weight (without the awn), central spikelet dry weight (without the awn), lateral spikelet dry weight (without the awn) were measured. Due to the small size of structures at the AP, GrA, and YA stages, dry weight was not determined at any of these three stages.

Tissue preparation and mRNA sequencing

The spikes of 17 stages were frozen in liquid nitrogen, ground into powder, and total RNA was extracted using TRIzol reagent (Invitrogen), treated with DNase I, and purified using RNeasy columns (QIAGEN). A total of 1 μg total RNA per sample was used as input material for the preparation of sequencing libraries using Next Ultra RNA Library Prep Kit for Illumina (NEB, USA) following the manufacturer's recommendations. Index codes were added to attribute sequences to each sample following sequencing and demultiplexing. The clustering of index-coded samples was performed on a cBot Cluster Generation System using a TruSeq PE Cluster Kit v3-cBot-HS (Illumina) according to the manufacturer's instructions. After cluster generation, the libraries were sequenced on an Illumina Novaseq platform and 150-bp paired-end reads were generated and analyzed.

Read mapping and differential gene expression analysis

The reference genome used here was the barley genome (International Barley Sequencing Consortium (IBSC), 2016) downloaded from https://galaxy-web.ipk-gatersleben.de/libraries/folders/F5969b1f7201f12ae. The quality of raw data was assessed using Fastqc[89] (http://www.bioinformatics.babraham.ac.uk/projects/fastqc/). Raw RNA-seq reads were processed to remove low-quality reads using trimmomatic.[90] The software tool Salmon[91] and the Tximport package in R[92] were used to quantify RNA-seq data and import transcript-level quantifications from Salmon and optionally aggregate them to gene levels for differential expression analysis. Raw read counts were normalized to transcripts per million (TPM) expression levels.

Differentially expressed genes (DEGs) throughout the reproductive period (AP-36DFL)

DEGs were identified by comparing time courses for each of the 17 developmental time points at each position using ImpulseDE2 (v1.6.1) in R.[93] ImpulseDE2 was used in case-only mode and no batch effects settings were added to the parameters. Identification of DEGs was according to false discovery rate (FDR)-adjusted p-values below 0.05. A total of 15,127 DEGs were identified from the same genes between the five positions time points different genes.

Differential expression of genes in the top, middle and bottom positions during the same developmental stage

Barley inflorescences are continuously growing; however, the apical inflorescence degenerates at certain stages during barley development. The DESeq2 R package[94] was used to identify DEGs ($log_2FC > 1$ or $log_2FC < -1$ and FDR-adjusted p-values < 0.05) between the top and middle positions or between the bottom and middle positions of the inflorescence.

Clustering of gene expression profiles and GO enrichment analysis

A total 9,228 DEGs with TPM were clustered using Mfuzz[95] into 15 significant discrete clusters. The TPM for each gene was determined from the mean values of three biological replicates. GO term enrichment analysis in each gene cluster was performed using Eggnog Mapper[96] and the -i Barley_Morex_V1.fasta -d virNOG -m diamond settings to find the GO category corresponding to each set of genes, using the R package clusterProfiler[97] for GO enrichment. The significance of enrichment was estimated using an FDR-adjusted p-value < 0.05.

Weighted gene co-expression network analysis (WGCNA)

The first step was to acquire data for each of the three biological replicates for each time point/position. TPM data were obtained using 255 tissue samples (17 stages × 5 positions × 3 replicates), and data for all genes were used for co-expression network construction, module detection, module-traits relationship determinations, and identification of hub genes from the interesting modules. Co-expression network modules were identified using average TPM values and the WGCNA package[98] in R. In the spike length-increasing stages (AP to LHD), genes with a low coefficient of variation for average TPM (CV < 0.25) among all sample types (5 different positions, 17 points) were discarded and the remaining 9,117 genes were used for analysis. The co-expression modules were obtained using theTOMtype parameter unsigned, and a Pearson correlation matrix was calculated between all pairs of selected genes from which an adjacency matrix was constructed by raising the correlation matrix to the power of nine (Figure S2A) The minModuleSize parameter was 50, and the modules were identified using the Dynamic Hybrid Tree cut algorithm, with mergeCutHeight set to 0.25. A total of 8 modules (Figures S2B and S2C) were identified for spike length from the WGCAN results. For hub gene identification, a weight value greater than 0.4 was selected for connectivity in the positive correlation module as the hub gene. In the spike weight-increasing stages (LHD to 32DFL), the coefficient of variation on average TPM (CV < 0.25) was first calculated among all sample types (5 × 17), yielding a power value of more than 30, prompting us to raise the coefficient of variation (CV < 0.7) among all sample types (5 × 17); the remaining 3,995 genes were used for analysis. The co-expression modules were obtained using the TOMtype parameter unsigned and a Pearson correlation matrix was calculated between all pairs of selected genes from which an adjacency matrix was constructed by raising the correlation matrix to the power of 18 (Figure S3A) The minModuleSize was set to 50; the modules were identified using the Dynamic Hybrid Tree cut algorithm, and mergeCutHeight was 0.25. A total of 8 modules (Figures S3B and 5E) were identified for spike length from the WGCAN results. Furthermore, relative TPM values were averaged to summarize expression patterns within individual modules. A module eigengene (ME) value summarizes the expression profile of a given module as the first principal component. For hub gene identification in the brown module, genes were selected with absolute correlation values greater than 0.8 for both the gene and module and spike weight traits. The networks were visualized using Cytoscape3.7.1.[99]

Mutant identification

The mutant of *HvGELP96* was obtained from an ethyl methanesulfonate (EMS)-mutagenized population library in the barley landrace ''Hatiexi'' (HTX), which was a spring-type, hulled barley whose entire body turns black when the plants reach full maturity. The HTX genome and Morex genome were highly collinear.[77] TILLING (targeting induced locus lesion in genomes) technology and the assembled HTX genome were used to identify the mutant of *HvGELP96* gene.[77] Homozygous M4 plants were harvested for phenotyping. To validate the genotype of the mutant, genomic DNA was extracted from the leaves of individual plants. The region encompassing the target site was amplified by PCR using genomic DNA as template. Homozygous mutants were identified via sequence alignment after the PCR products were sequenced by Sanger sequencing. The primers used for mutant genotyping: forward primer, 5′-GTGATGG TAGCAGCCATGGTA-3'; reverse primer, 5′-CGGATGCTACTGGCACACTAA-3'.

QUANTIFICATION AND STATISTICAL ANALYSIS

R software (v 3.5.3) was used for data analysis. The data are presented as mean ± SD. Statistical analyses were performed using a paired two-tailed Student's t-test (*p < 0.05, **p < 0.01, ***p < 0.001) for comparisons between two groups. Details about the statistical analyses are described in the method and figure legends.